Catal Lett (2016) 146:1373–1396
DOI 10.1007/s10562-016-1755-0

Some New Nano-sized Mononuclear Cu(II) Schiff Base Complexes: Design, Characterization, Molecular Modeling and Catalytic Potentials in Benzyl Alcohol Oxidation

Laila H. Abdel-Rahman[1] · Ahmed M. Abu-Dief[1,2] · Mohamed Shaker S. Adam[1,3] · Samar Kamel Hamdan[1]

Received: 10 April 2016 / Accepted: 22 April 2016 / Published online: 18 May 2016

Abstract In the present contribution, some novel Cu(II) complexes were synthesized from tri- and tetradentate imine ligands. All the prepared compounds were elucidated by different physicochemical methods. Density Functional Theory calculations were carried out to explain the equilibrium geometry of the bsisnph and npisnph ligands and their Cu(II) complexes. Interaction of the synthesized ligands with Cu(II) affords nano-sized particles via TEM. The catalytic potentials of the prepared complexes has been tested within the oxidation of benzyl alcohol using an environmental friendly terminal oxidant, i.e. H_2O_2. The effect of various parameters, e.g. solvents, temperature and amount of catalyst was investigated. A mechanistic pathway of the catalytic oxidation was tentatively described and discussed.

Graphical Abstract

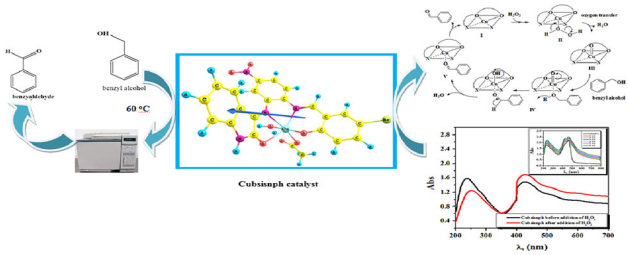

Keywords Cu(II) Schiff base complexes · TEM · Benzyl alcohol · Density Functional Theory · Catalytic activity · Hydrogen peroxide

1 Introduction

The oxidation of alcohols to corresponding carbonyls is a pivotal reaction synthetic organic chemistry [1, 2]. The most important applicability of the corresponding carbonyl compounds, i.e., benzaldehyde, is for the synthesis of fine chemicals such as fragrances or food additives [3]. Traditionally, oxidation of alcohols is carried out with stioichmetric Cr(VI) and Mn(VII) based oxidant [4] and it is found that a vast majority of such processes require the use of costly and toxic solvents [5]. Schiff base transition metal complex derivatives are the most attractive oxidation catalysts for alcohols and alkenes because of their cheap, easy synthesis, their chemical and thermal stability. Various studies have shown that the azomethine group have alone pair of electrons in either p or sp^2 hybridized orbital on nitrogen has biological and catalytic importance [6, 7]. Copper is copious metal on the earth's crust and is found in

Electronic supplementary material The online version of this article (doi:10.1007/s10562-016-1755-0) contains supplementary material, which is available to authorized users.

✉ Ahmed M. Abu-Dief
ahmed_benzoic@yahoo.com

[1] Chemistry Department, Faculty of Science, Sohag University, Sohag 82534, Egypt

[2] Departamento de Quimica Organica e Inorganica, Faculad de Quimica, Universdad de Oviedo, 33006 Oviedo, Spain

[3] Department of Chemistry, College of Science, King Faisal University, P.O. Box 380, Al Hufuf, 31982 Al Hassa, Saudi Arabia

various metalloproteins especially in enzymes contributed in the bounding of molecular oxygen or in moderate and highly selective oxidation transformations [8, 9]. Thus, it is surprising that only a few examples using cheap and "green" copper catalysts and molecular oxygen [10] or hydrogen peroxide are known so far [11–13]. Moreover, Copper compounds are well known as very remarkable reagent and catalyst in many organic reactions because of their stability and ease of handling [14]. From both an economic and environmental point of view, the quest for efficient catalytic systems that utilize clean, inexpensive primary oxidants such as molecular oxygen or hydrogen peroxide, i. e a green procedure for transforming alcohols to carbonyls compounds on an industrial scale remains an important challenge [15, 16].

Thus, our study stems to introduce the synthesis of new series of hexa-coordinated copper (II) complexes containing tri and tetradentate ligands [17]. Moreover, the characterization of copper complexes and their corresponding ligands was accomplished by a variety of physicochemical analysis. Copper(II) complexes have been effectively used as catalysts in oxidation of benzyl alcohol in presence of an aqueous hydrogen peroxide in various reaction parameter conditions.

2 Experimental

2.1 Materials and Reagents

All chemicals used in this study were obtained of the highest purity available.

2.2 Physical Measurements

Single crystal X-ray structure of npap ligand was recorded on Bruker–Nonius KappaCCD, equipped with a CCD detector and a liquid-nitrogen low-temperature. Melting points of the prepared ligands and decomposition temperatures of their copper complexes were determined using a Gallenkamp (UK) apparatus. NMR spectra of the ligands were recorded in Bruker ARX at 400.1 (^{1}H) and 100.6 (^{13}C) MHz using DMSO-d_6. A Perkin-Elmer 240c Elemental analyzer was used to micro-analytical data (C, H and N). Molar conductivities of the prepared Cu(II) complexes were determined in *N*,*N*'-dimethylformamide (DMF 1×10^{-3} M) at room temperature using Jenway conductivity meter model 4320. Magnetic measurements of the complexes were determined on Gouy's balance, the diamagnetic correction were made by Pascal's contents and $Hg[Co(SCN)_4]$ as a calibrant. The FT-IR spectra of the prepared samples were recorded on Shimadzu FTIR 8101 spectrophotometer using KBr discs. Electronic spectra of the prepared Schiff base ligands and their corresponding complexes were recorded on Jasco P- 530 UV–Visible spectrophotometer model T+80 using 10 mm matched quartz cells and data were reported in λ_{max}/nm. TGA analysis was recorded in dynamic flow of nitrogen atmosphere (40 cm^3/min) using Shimaduz cooperation 60H analyzer at heating rate 10 °C/min from ambient temperature to 750 °C. The absorbance of each complex was measured at different pH values. pH values were adjusted using a series of Britton universal buffer [18–20]. TEM images were recorded using a JEM-2100 microscope. The synthesized copper complexes were suspending in ethanol, followed by ultrasonication for 30 min. Then, a drop of the suspension was added to a carbon coated copper grid allowing the solvent to be evaporated before its introduction into the TEM. All the catalytic reactions (catalytic oxidation of benzyl alcohol) were carried out by Gas chromatography is computerized Agilent 5890A 19091 J-413: 325 °C equipped with a flame ionization detector and a HP-5 capillary column (phenyl methyl siloxane 30 m × 320 μm × 0.25 μm).

2.3 Synthesis of Schiff Base Ligands

npap ligand was synthesized by treatment of a stirred ethanolic solution (20 ml) of 2-hydroxy-1-napthaldehyde (5 mmol, 0.86 g) with 2-aminopyridine (5 mmol, 0.47 g). The reaction mixture was kept under stirring and refluxing for 1 h (at 70 °C). After cooling, yellow crystals were observed which filtered off and washed many times with ethanol. The ultimate product (npap) was obtained in a pure form by recrystallization with ethanol [20]. Yellow crystals; m.p.: 170 °C; yield (88 %). ^{1}H NMR (400 MHz, DMSO-d_6): δ = 6.86 (d, 1H, ArH naphthyl, ^{3}J = 9.3 Hz), 7.36–7.30 (m, 2H, ArH naphthyl), 7.54 (t, 1H, ArH naphthyl, ^{3}J = 8.1, 7.3 Hz), 7.63 (d, 1H, ArH naphthyl, ^{3}J = 8.0 Hz), 7.74 (d, 1H, ArH naphthyl, ^{3}J = 7.7 Hz), 7.90 (d, *m*-pyH, 1H, ^{3}J = 9.4 Hz), 7.95 (dt, 1H, *p*-pyH, ^{4}J = 1.4, 1.7 Hz, ^{3}J = 7.4, 7.7 Hz), 8.26 (d, 1H, *m*-pyH, ^{3}J = 8.3 Hz), 9.85 (s, 1H, CH=N, ^{4}J = 0.7 Hz, ^{3}J = 4.5 Hz), 15.19 ppm (s, 1H, OH, ^{3}J = 8.0 Hz); ^{13}C NMR (100 MHz and DEPT135, DMSO-d_6): δ = 108.6 (C_q, C–CH=N), 115.8 (CH), 120.1 (CH), 122.0 (CH), 124.3 (CH), 124.4 (CH), 127.0 (C_q, naphthyl), 129.1 (CH), 129.6 (CH), 134.1 (C_q, -OH), 139.3 (CH *m*-py), 139.5 (CH *m*-py), 149.4 (CH *p*-py), 151.5 (CH, *o*-py), 153.6 (C_q-py), 176.9 ppm (CH, CH=N).

According to a reported method for the synthesis of bsisnph and npisnph ligands [21], a 4-nitro-*o*-phenylenediamine (5 mmol, 0.77 g) in ethanol (25 ml) was slowly added to an ethanolic solution (25 ml) of isatin (5 mmol, 0.74 g). It was followed by a slow addition of 5- bromosalicylaldehyde (5 mmol, 1.00 g) or 2-hydroxy-1-

napthaldehyde (5 mmol, 0.86 g) solution in 25 ml ethanol (for synthesis of bsisnph or npisnph, respectively). The reaction mixture was kept under refluxing for 3 h. A colored precipitate was observed which filtered off and washed thoroughly with an aqueous ethanol solution (1:1). The final product was dried in desiccator over anhydrous calcium chloride. The purity of bsisnph or npisnph was checked by TLC, which is quit pure and was not need for further purification.

For bsisnph, ^{1}H NMR (400 MHz, DMSO-d6): δ = 11.61 (s, 1H, OH), 8.94 (s, 1H, =CH), 7.56 (s, 1H, NH), 8.11(s, 1H, H-C6, o-NO_2), 7.95 (d, 2H, ArH), 7.62–6.65 (d, 2H, ArH, 5-bromosalicyaldehyde) 7.91 (s, 1H, H-C7, isatin), 6.81–6.77 (t, 3H, H-C6, isatin).

For npisnph, ^{1}H NMR (400 MHz, DMSO-d6): δ = 14.58 (s, 1H, OH), 10.82 (s, 1H, CH=N), 9.76 (s, 1H, H-C6, *o*-NO2), 8.64–8.19 (d, 2H, ArH), 8.94–7.99 (d, 4H, naphthyl), 6.67 (s, 2H, naphthyl) 7.91 (d, 1H, H-C7, isatin), 7.60–7.23 (t, 3H, H-C6, isatin), 7.25 (s, 1H, NH).

2.4 Synthesis of Schiff Base Cu(II) Complexes

An ethanolic solution (30 ml) was charged with copper acetate monohydrate (5 mmol, 1.00 g) and npap ligand (10 mmol, 2.48 g). The resulting mixture was stirred for 3 h at room temperature. An observed dark green precipitate was filtered off, washed various times with ethanol and then dried in vacuum over anhydrous calcium chloride. The final pure Cunpap complex was obtained by recrystallization with hot ethanol. Green solid; m.p. > 300 °C; yield (77 %).

Similarly for the synthesis of Cubsisnph and Cunpisnph complexes, an ethanolic solution (30 ml) was charged with copper acetate monohydrate (5 mmol, 1.00 g) and bsisnph ligand (5 mmol, 2.32 g) or npisnph ligand (5 mmol, 2.18 g). The color of the complexes changed immediately after mixing. The resulting mixture was refluxed under stirring for 1 h (at 50 °C). After cooling, solvent was removed under vacuum and the collected precipitate was thoroughly washed with ethanol and desiccated over anhydrous calcium chloride. The final pure Cubsisnph and Cunpisnph complexes were obtained by recrystallization with hot ethanol.

2.5 X-ray Crystallography

The suitable crystals of npap ligand for X-ray analysis were obtained by recrystallization from ethanol by slow evaporation. The structure was solved by using the program(s): SHELXS86 [22–24]; program(s) used to refine structure: CRYSTALS [25]; molecular graphics: CAMERON [26]; software used to prepare material for publication. A summary of the key crystallographic information is given in Table S1. The selected bond lengths and bond angles are listed in Table S1.

2.6 Magnetic Moment Measurements

Magnetic moment measurements are greatly used in studying transition metal complexes. Magnetic Susceptibility calculated at room temperature according to the following form [27]:

$$\mu_{\text{eff}} = 2.83\sqrt{\chi'_M T} \quad (1)$$

$$\chi'_M = \chi_M - (\text{diamag. Corr.}) \quad (2)$$

where μ_{eff}, is the magnetic moment (in Bohr Magneton), χ'_M is molar magnetic susceptibility, T is the absolute temperature (K) and χ_M is molar magnetic susceptibility after correction.

2.7 Evaluation of the Stoichiometry of the Schiff Base Ligands Complexes

The stoichiometry of the tested complexes were determined by applying the spectrophotometric the molar ratio method [17–20] and the continuous variation method [18, 19, 28], as shown in Figs. 3 and 4.

2.8 Evaluation of the Apparent Formation Constants of the Synthesized Complexes

The apparent formation constants (K_f) of the synthesized complexes formed in solution were determined from spectrophotometric measurements using the continuous variation method [17–20], according to the following relations. The obtained K_f values (Table 1) indicate the stability of these complexes.

For Cunpap complex

$$K_f = \frac{A/A_m}{4C^2\left(1 - A/A_m\right)^3} \quad (3)$$

For Cubsisnph and Cunpisnph complexes

$$K_f = \frac{A/A_m}{(1 - A/A_m)^2 C} \quad (4)$$

where A is the arbitrary chosen absorbance values on either side of the absorbance mountain col (pass), C is the initial concentration of the metal, and A_m is the absorbance at the maximum formation of the complex.

2.9 Kinetic Studies for the Prepared Complexes

The decomposition and thermal dehydration of the mentioned complexes were studied kinetically using the integral method applying the Coats–Redfern method. The thermodynamic activation parameters of decomposition processes of dehydrated complexes namely activation energy (E^*), frequency factor (A), entropy of activation

Table 1 Analytical and physical data of the Schiff base ligands and their corresponding complexes

Compounds	Λ_m (Ω^{-1} cm^2 mol^{-1})	μ_{eff} (B. M.)	Elemental analysis, Found(calcd.) (%)			Electronic spectra (in DMF)			Stability constant		
			C	H	N	λ_{max} (nm)	ε_{max} (dm^3 mol^{-1} cm^1)	Assign.	K_f	$\log K_f$	$\Delta(G^*)$
npap	–	–	77.35	4.79	11.32	391	1411	$n \rightarrow \pi^*$	–	–	–
			(77.42)	(4.84)	(11.29)	427	1252	$n \rightarrow \pi^*$			
Cunpap	7.42	2.18	65.60	4.17	9.50	322	1418	Intraligand	1.34×10^{12}	12.13	−69.18
			(65.69)	(4.28)	(9.58)	464	2318	LMCT			
						644 (b)	753	d–d			
bsisnph	–	–	54.15	2.74	11.99	389	1463	$n \rightarrow \pi^*$	–	–	–
			(54.21)	(2.80)	(12.05)	443	1573	$n \rightarrow \pi^*$			
Cubsisnph	3.65	2.10	45.62	2.75	9.17	321	962	Intraligand	4.44×10^5	6.56	−37.44
			(45.66)	(2.82)	(9.27)	483	1463	LMCT			
						695	149	d–d			
						746	136	d–d			
npisnph	–	–	68.69	3.55	12.73	314	840	$\pi \rightarrow \pi^*$	–	–	–
			(68.81)	(3.67)	(12.85)	396	984	$n \rightarrow \pi^*$			
						460	1180	$n \rightarrow \pi^*$			
Cunpisnph	4.46	1.87	54.48	3.60	9.31	393	1094	Intraligand	8.24×10^5	5.92	−33.73
			(54.59)	(3.71)	(9.44)	484	1484	LMCT			
						515	1317	d–d			
						737	550	d–d			

(ΔS), enthalpy of activation (ΔH), and free energy change of the decomposition (ΔG) are estimated graphically from TGA data by employing the Coats–Redfern relation [17, 20, 29] in the following form:

$$\log\left[\frac{\log(w_\infty/(w_\infty - w)}{T^2}\right] = \log\left[\frac{AR}{\varphi E^*}\left(1 - \frac{2RT}{E^*}\right)\right] - \frac{E^*}{2.303RT} \quad (5)$$

where is w_∞ the mass loss at the completion of the decomposition reaction, w is the mass loss up to temperature T, R is the universal gas constant and ϕ is the heating rate. Since $1\text{-}2RT/E^* \approx 1$, the plot of the left-hand side of equation versus 1/T gives a straight line whose slope (E^*/R) and the pre-exponential factor (A) can be determined from the intercept. The other kinetic parameters; the entropy of activation (ΔS^*), enthalpy of activation (ΔH^*) and the free energy change of activation (ΔG^*) were calculated using the following equations:

$$\Delta S^* = 2.303R \log \frac{Ah}{KBT} \quad (6)$$

$$\Delta H^* = E^* - RT \quad (7)$$

$$\Delta G^* = H^* - T\Delta S^* \quad (8)$$

where K_B is Boltzmann's constant and h are Plank's constant. The results of kinetic parameters for the studied complexes are summarized in Table 2.

2.10 Molecular Modeling

Since single crystal X-ray structure for bsisnph and npisnph ligands and their copper complexes was not available, so, quantum chemical calculations were utilized to find the geometrically optimized structures of these complexes. Optimization of geometries was carried out by the density functional theory method (DFT) using the Gaussian09 program package [30]. Density Functional Theory (DFT) used at the B3LYP level [31], 6-311G* [32, 33] as a basis set for the ligand and LANL2DZ as a basis set for the complexes.

3 Catalytic Activity

3.1 Procedure for Catalytic Oxidation

Catalytic oxidation of benzyl alcohol to corresponding aldehydes and ketones by the titled copper complexes were studied in the presence of H_2O_2. In a typical reaction, benzyl

Table 2 Thermal decomposition steps, mass loss (%), proposed lost segments, final residue thermo-kinetic activation parameters of each decomposition step for metal complexes

Complex	Decomp. temp. (°C)	Mass loss (%)		Proposed segment	E^* (KJ mol^{-1})	A × 10^4 (S^{-1})	ΔH^* (KJ mol^{-1})	ΔG^* (KJ mol^{-1})	ΔS^* (J mol^{-1} K^{-1})
		Found	(Calcd.)						
Cunpap	31–116	4.61	(4.64)	1.5 H_2O	0.09	0.82	−0.59	12.51	−159.30
	116–274	18.21	(17.93)	$C_6H_5N_2$			−1.92	39.22	−170.00
	275–528	66.62	(66.43)	$C_{26}H_{17}N_2O_2$			−2.91	57.32	−170.00
Residue	>528	10.54	(11.03)	Cu			–	–	–
Cubsisnph	27−207	3.32	(2.98)	H_2O	0.12	0.66	−0.24	6.44	−155.76
	207–308	9.81	(9.76)	CH_3Coo			−1.96	44.43	−170.40
	308–392	32.78	(32.74)	C_7H_4NOBr			−2.31	47.92	−171.73
	392–502	20.00	(19.97)	$C_6H_3NO_2$			−2.78	57. 50	−173.17
	502–749	24.02	(23.99)	$C_8H_5N_2O$			−3.51	72.85	−175.05
Residue	>749	10.55	(10.05)	Cu			–	–	–
Cunpisnph	24–120	3.05	(3.03)	H_2O	0.11	0.71	−1.06	22.43	−166.92
	120–215	3.06	(3.03)	H_2O			−1.36	28.75	−169.65
	215–367	9.96	(9.94)	CH_3COO			−2.22	45.87	−170.78
	367–513	28.50	(28.47)	$C_{11}H_7NO$			−3.33	68.71	−173.97
	459–749	44.90	(44.82)	$C_8H_5N_2O$ + $C_6H_3NO_2$			−3.78	78.14	−174.99
Residue	>749	10.53	(10.71)	Cu	–	–	–	–	–

alcohol (0.1 cm^3, 1.0 mmol) was added to a solution of copper complexes (Cunpap, Cubsisnph, Cunpisnph) contacted to air (0.05 mmol) in 10 ml of acetonitrile at 50, 60, 70, 80 or 90 °C in an water bath under magnetic stirring. The reaction was initiated by charging with 5.54 mmol aqueous H_2O_2 (30 %) at the typical temperature. The reaction was monitored by gas chromatographic analyses, using computerized standard calibration curve. The oxidation products were identified by comparing their retention times with those of authentic samples. Control reactions were done by withdrawing samples (ca. 2 ml) of the reaction mixture and treatment of the reaction mixture with solid MnO_2 (to quench the excess aqueous H_2O_2) and with anhydrous sodium sulfate (to absorb excess water molecules), under the same conditions in the catalytic runs. The resulting slurry was filtered on Celite, and the filtrate was injected in the GC. This allowed independent measurements for each sample. The chemo-conversion of benzoyl alcohol to benzaldehyde was calculated according to computerized standard calibration curves. All the oxidation processes were run at least in duplicate to confirm the yield of the products.

4 Results and Discussion

4.1 Characterization of the Prepared Schiff Base Ligands

npap ligand was synthesized via common condensation of 2-hydroxy-1-napthaldehyde with 2-aminopyridine in 1:1 molar ratio (Scheme 1) [20]. On the hand, bsisnph and npisnph ligands were prepared via reaction of 4-nitro-*o*-phenylenediamine, isatin and 5-bromosalicyaldehyde or 2-hydroxy-1-napthaldehyde [21]. The structure of npap ligand was elucidated using single crystal X-ray analysis, micro analytical, spectroscopic measurements.

4.1.1 Crystallography

Single crystal X-ray analysis shows npap ligand belongs to monoclinic crystal system, space group $P12_1/c_1$. Figure 1a, b shows the ORTEP diagram with atomic numbering scheme and close packing structure for npap compound. Details of crystallographic parameters, data collection and refinements are listed in Table S1. Selected bond lengths (Å) and angles (°) for npap ligand are listed in Table S2. The bond lengths of N(5)–C(4) and N(27)–C(28) are1.295 (6) and 1.308(4) Å, respectively for npap compound which correspond to typical double bond characteristic. Bond angles C(26)–N(27)–C(28), 120.3(5); C(6)–N(5)–C(4), 122.5(6) and O(20)–C(1)–C(29), 120.7(5) for npap compound were also found.

4.1.1.1 ^1H NMR Spectra The synthesized ligands were characterized by the ^{1}H NMR (400 MHz and δ/ppm) in DMSO-d_6. The ^{1}HNMR spectra of the synthesized Schiff base ligands showed the distinguished NMR signals. The ^{1}HNMR spectra of the prepared npap show singlet due to hydrogen bond –OH proton at 15.19 ppm [34, 35]. The higher values of δ for the –OH group can be assigned to the

Structure of Schiff base ligand		Structure of Cu(II) Schiff base complexes	
npap	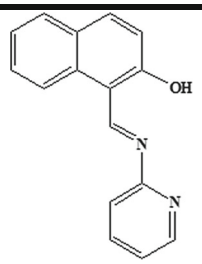	Cunpap	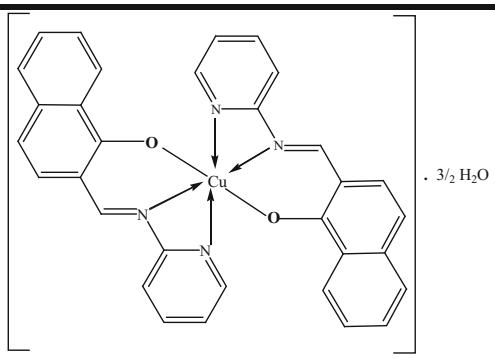
bsisnph	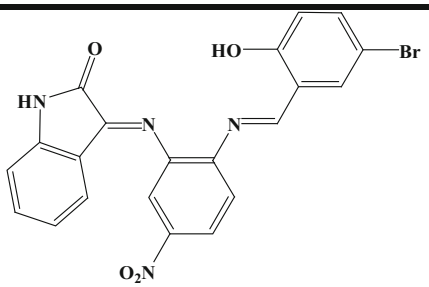	Cubsisnph	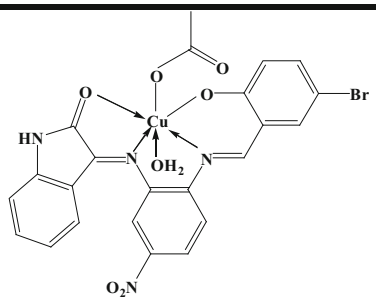
npisnph	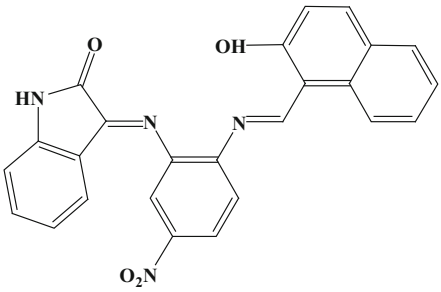	Cunpisnph	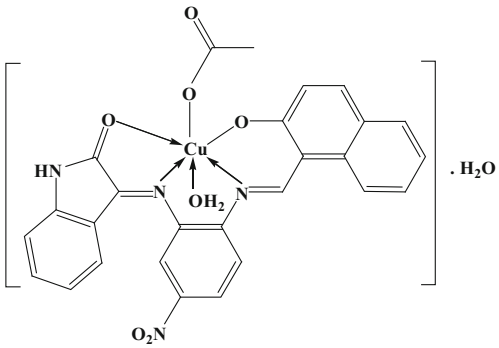

Scheme 1 The proposed structure of the Schiff base ligands and their corresponding complexes

presence of intramolecular hydrogen bonding [36]. The characteristic proton of azomethine appeared at 9.82 ppm. The signals of CH pyridine are found at 8.26 and 7.90 ppm. Aromatic protons of naphthyl ring found in the range of 7.74–6.86 ppm are assigned to aromatic protons. It was noticed that DMSO did not have any coordinating effect on the prepared ligands. The ^{1}H NMR spectrum of bsisnph imine ligand exhibited singlet singal at 11.61 ppm for (–OH) group. The signal due to the azomethine proton (–HC=N) is found to be at $\delta = 8.94$ ppm. The signals due to aromatic protons of 5-bromosalicyaldehyde and 4-nitro-o-phenylenediamine have resonated as doublet in the region of 8.11–6.65 ppm. The proton of the amide "NH" group appeared as singlet at 7.56 ppm. The signals are due to isatin protons as doublet at 7.91 ppm and triplet in the region 6.81–6.77 ppm.

In the ^{1}HNMR spectrum of npisnph imine ligand displayed singlet singal at 14.58 ppm due to the proton of OH group. The singal due to azomethine proton resonated at 10.82 ppm. The signals due to aromatic protons of napthyl and 4-nitro-ophenylenediamine have resonated as multiplets in the region of 9.76–7.99 ppm. The proton of the amide "NH" group appeared as singlet at 7.25 ppm. The signals due to isatin protons as doublet at 7.91 ppm and triplet in the region 7.43–6.67 ppm. The ^{1}H NMR spectra

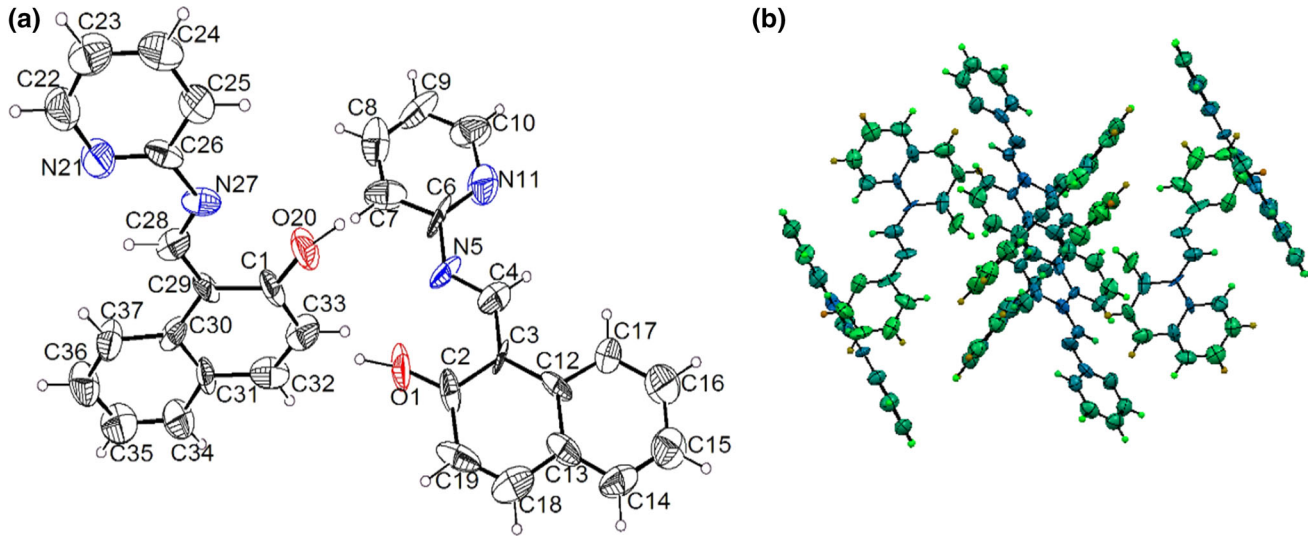

Fig. 1 **a** An ORTEP drawing of npap with the atom-numbering. **b** Molecular packing and hydrogen bonding interactions of npap

of the complexes cannot be obtained due to interference in their paramagnetic properties.

4.1.1.2 ^{13}C NMR Spectroscopy ^{13}C NMR spectral data were consistent with ^{1}H NMR spectral data. The ^{13}CNMR spectra of the npap ligand have showed a peak at 176.9 ppm due to characteristic azomethine carbon. The ligand also exhibited signals at 108.6 (C_q, C–CH=N), 115.8 (CH), 120.1 (CH), 122.0 (CH), 124.3 (CH), 124.4 (CH), 127.0 (C_q, napthyl), 129.1 (CH), 129.6 (CH), 134.1 (C_q, -OH), 139.3 (CH *m*-py), 139.5 (CH *m*-py), 149.4 (CH *p*-py), 151.5 (CH, *o*-py), 153.6 (C_q-py).

The ^{13}C NMR of bsisnph Schiff base ligand displayed resonance signals at 250.0 ppm, corresponding to carbonyl group. Two (C=N) groups of the Schiff base ligand appeared at 176.0 ppm (CH, CH=N), 208.2 (C_q=N). The resonance signals observed at $\delta = 110.8$ (C_q), 112.7 (C_q), 113.7 (CH), 114.6 (CH), 119.4 (CH), 123.1 (C_q), 124.7 (CH), 133.2 (CH), 134.1 (C_q), 135.9 (CH), 136.8 (C_q), 138.8 (C_q), 150.6 (C_q–N=C), 158.9 (C_q-OH), 159.9 (CH) due to the aromatic carbons.

The spectrum of npisnph ligand has showed a peak at 234.7 ppm displayed a peak due to (C=O) group. In addition, the azomethine (C=N) carbon exhibited its peaks at 168.00 ppm (CH, CH=N) and 181.80 ppm (C_q=N). The aromatic carbons of ligand show signals at $\delta = 110.5$ (C_q), 113.9 (CH), 116.2 (C_q), 120.0 (CH), 121.6 (CH), 124.1 (CH), 124.4 (CH), 127.9 (C_q), 128.5 (CH), 129.3 (CH), 133.1 (CH), 133.3 (C_q), 137.3 (C_q), 149.8 (C–N=C), 161.0 (CH), 163.7 (C_q-OH), 167.2 (C_q),. This confirms the formation of Schiff base ligand.

4.2 Characterization of the Prepared Metal Complexes

The metal complexes are solids, stable in air and partially soluble in ethanol but entirely soluble in, acetonitrile, acetone, DMF and DMSO. The structural characteristics of metal complexes were elucidated by employing elemental analysis, UV–Vis., IR and TGA.

4.2.1 Microanalyses and Molar Conductance Measurements

The microanalyses results of the studied Schiff base ligands and their complexes are given in Table 1 and suggested that npap Schiff base ligand act as tridentate (ONN) and form complexes in 1: 2 ratio metal to ligand, while bsisnph and npisnph ligands act as tetradentate (ONNO) and form complexes in 1: 1 ratio metal to ligand. Magnetic susceptibility measurements values of the prepared Schiff base copper complexes are (1.87–2.18 B.M.) which suggests octahedral geometry [37, 38]. The conductivity measurement has frequently been used in structure elucidation of metal chelate i.e. the possible mode of bonding within the limit of their solubility; they also provide a method of testing the degree of ionization of the complexes. The molar conductance values are found to be in the range 3.65–7.42 Ω^{-1} mol^{-1} cm^2, indicating the non-electrolytic nature of the complexes [39]. The non-electrolytic nature of the prepared complexes can be accounted by the deprotontation of the phenolic group of the ligand when it is coordinated to metals and presence of acetate ion

inside the coordination sphere, in case of Cubsisnph and Cunpisnph complexes. The suggested structure of Schiff base ligands and their corresponding metal complexes are found in Scheme 1.

4.2.2 Infrared Spectra

The coordination way and sites of the ligands to the metal ions were investigated by comparing the infrared spectra of Schiff base ligands with their metal complexes (cf. Table S3). The characteristic phenolic (OH) mode due to the 5-bromosalicyaldehyde or hydroxyl group of 2-hydroxy benzaldehyde moiety, present in the Schiff base ligand was observed at 3426–3464 cm^{-1} [40]. The absence of this band in all the complexes indicates the deprotonation of hydroxyl group. This facts further supported by the decrease in the absorption frequency of phenolic υ(C–O) from 1212 and 1315 cm^{-1} in the free ligands to 1172–1285 cm^{-1} in the metal complexes confirming the other coordination site of Schiff base is the phenolic oxygen [41]. In the case of metal complexes, there are number of medium-to- weak bands in the two range (535–641 cm^{-1}) and (442–581 cm^{-1}) are assigned to the stretching frequencies of the υ(M–O) and υ(M–N) bands, respectively. The IR spectrum of the npap Schiff base ligand show bands at 1630, 1585 cm^{-1}, which is assigned to azomethine υ(CH=N) linkage and pyridine (C=N) stretching vibrations [17–20, 42]. On other hand, bsisnph and npisnph Schiff base ligands exhibited bands at the region 1607–1627 cm^{-1}, 1599–1634 cm^{-1} due to asymmetric nature [43]. These bands are shifted to lower frequencies in the spectra of their metal complexes compared with the above Schiff base ligands denoting the involvement of the azomethine nitrogen in chelation with the metal ion, the coordination of nitrogen to the metal ion could be expected to minify the electron density of the azomethine link and thus caused shift in the (C=N) group [44]. In (bsisnph, npisnph) Schiff base ligands and their copper complexes show an intense peak at 3196–3199 cm^{-1} which is a characteristic feature of NH stretching frequency [45]. The stretching vibration motion of indole (C=O) in the (bsisnph, npisnph) free ligands located at 1736–1740 cm^{-1}, which is shifted to lower frequencies in the spectra of the complexes indicating the involvement of (C=O) in complexation [46]. Two essential strong to medium bands were found at 1569–1589 and 1341–1365 cm^{-1} which could be assigned to (υ_{asy} COO) and (υ_{sy} COO) vibrations of carboxylate ion [47]. The difference between the asymmetric and symmetric stretching vibration motions $\upsilon[(\upsilon_{asy}\ COO) - (\upsilon_{sy}\ COO)]$ was found 200 cm^{-1}, which was matched with monodentate ligation [48]. These complexes also show weak bands at 820–840 cm^{-1} due to presence of rocking mode of coordinated water molecules [49, 50]. The presence of coordinated water was also established and supported by TGA analysis of these complexes.

4.2.3 Electronic Spectra

In this part, we would like to clarify the important role played by electronic spectra in determining the geometrical structures of the investigated metal complexes. The electronic spectra of the free ligands and the complexes were carried out in DMF solution (cf. Table 1; Fig. 2). The absorption band below 314 nm is assigned to $\pi \rightarrow \pi^*$ transition within the aromatic ring. The absorption band noticed in all ligands spectra within the range of 389–396 nm is most probably due to $n \rightarrow \pi^*$ transition for the electrons localized on the (C=N) chromophore [51]. The third band at $\lambda_{max} > 400$ nm involves $n \rightarrow \pi*$ transitions of the donating groups [52]. On complexation this band disappeared suggesting the coordination of azomethine nitrogen to the metal ion, as the formation of the metal–nitrogen bond stabilizes the electron pair on the nitrogen atom [53]. Thus addition of metal ion to the ligand solution causes characteristic changes in the visible absorption spectra of the ligand, suggesting an immediate complex formation in solution [54]. The designed complexes display a characteristic band centered at $\lambda_{max} = 321–393$ nm, due to an intramolecular charge transfer transition taking place in the complexed ligand. Moreover, there is a band shown in the region 464–484 nm, which can be attributed to charge transfer from ligand to metal. Electronic spectra of Cunpap complex exhibited band at 644 nm assignable to a $^2E_g \rightarrow {}^2T_g$ transition characteristic of octahedral geometry [55, 56]. Cubsisnph and Cunpisnph complexes show bands at 737–747 nm, 512–695 nm a $^2E_g \rightarrow {}^2T_g$ transition characteristic of octahedral geometry [57].

4.2.4 Evaluation of the Stiochmetry of the Prepared Schiff Base Complexes

The stoichiometry of the tested complexes was determined by applying the spectrophotometric continuous variation [17–20, 23, 34, 35] and molar ratio methods [26, 36–38]. The curves of continuous variation and molar ratio methods were used for the determination of chelation stoichiometry. The curves of continuous variation methods displayed maximum absorbance at mole fraction $X_{ligand} = 0.56$ in Cubsisnph and Cunpisnph complexes, which indicates the formation of complex with metal ion to ligand ratio 1: 1 as presented in Scheme 1. In the case of Cunpap complex, maximums of absorbance at mole fraction at $X_{ligand} = 0.65–0.70$ implicates a 1: 2 (metal ion to ligand) molecular association. Moreover, the data resulted from applying the molar ratio method assist the same metal ion to ligand ratio of the prepared complexes (Figs. 3, 4).

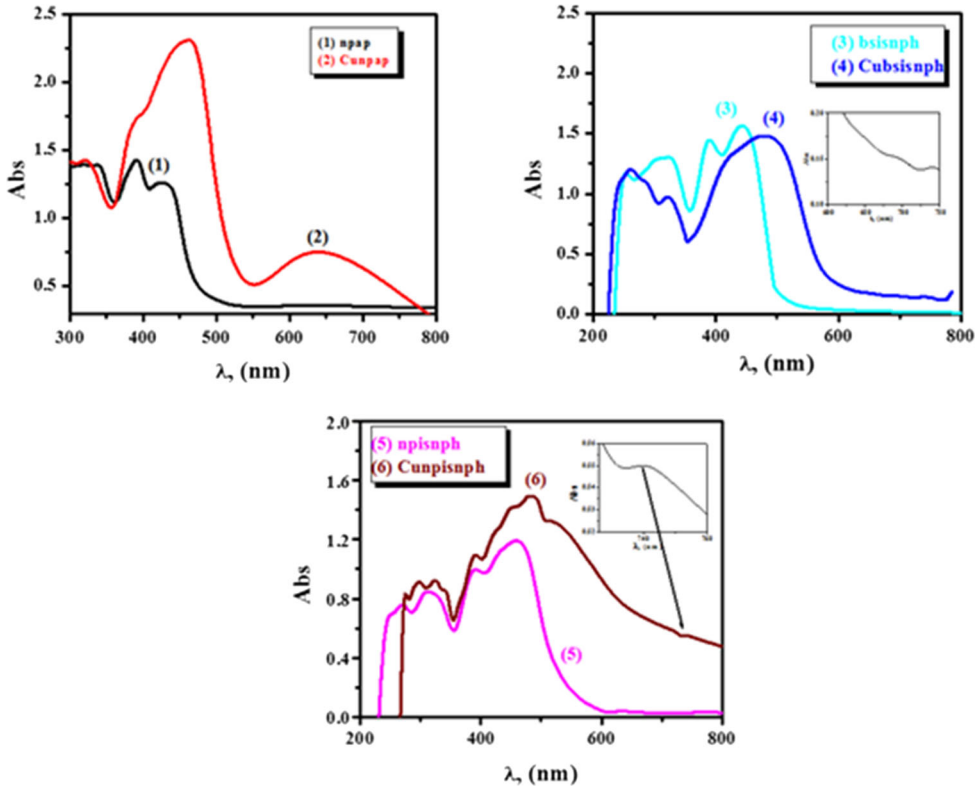

Fig. 2 Molecular electronic spectra of (1) [npap] = (2) [Cunpap] = (3) [bsisnph] = (4) [Cubsisnph] = (5) [npisnph] = (6) [Cunpisnph] = 10^{-3} M

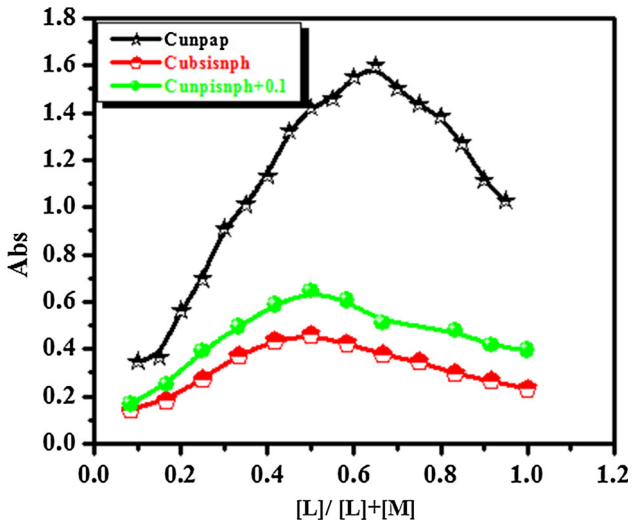

Fig. 3 Continuous variation plots for the prepared complexes in aqueous ethanolic medium at [Cunpap] = [Cubsisnph] = [Cunpisnph] = 10^{-3} M and 298 K

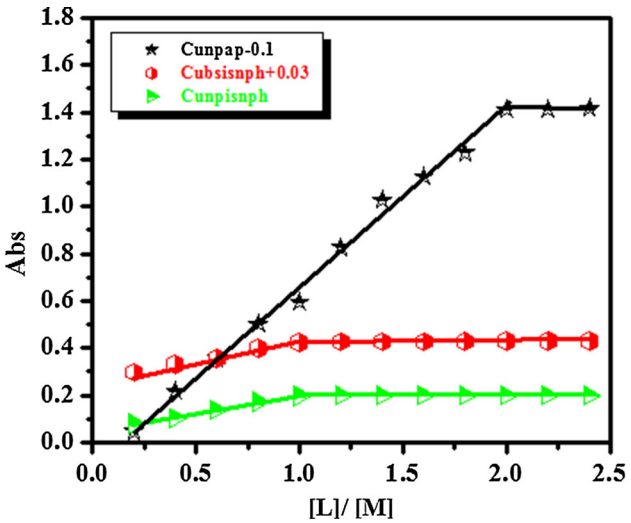

Fig. 4 Molar ratio plots for the studied complexes in aqueous–ethanolic mixture at [Cu] = 10^{-3} M, [npap] = [bsisnph] = [npisnph] = 10^{-3} M and 298 K

4.2.5 Evaluation of the Apparent Formation Constants of the Synthesized Complexes

The obtained the apparent formation constants values indicate the high stability of the prepared complexes. The values of (K_f) for the prepared complexes increase in the following sequence: Cunpap > Cunpisnph > Cubsisnph. Moreover, the values of log K_f (stability constant) and Gibb's free energy (ΔG^*) of investigated complexes are cited in this Table 1. The negivate values of Gibbs free energy illustrated that the coordination of the investigated ligands with Cu(II) is spontaneous and favorable.

4.2.6 Determination of Stability Range of the Investigated Complexes

The stability range of the studied complexes was found to be in the range pH 4–10 for npisnphCu complex, pH 5–10 for Cunpap and Cubsisnph complexes, according to the obtained pH absorbance curves (Fig. 5).This means that Cu (II) ion greatly stabilizes the tested Schiff base ligands in this range. Accordingly, these ligands can be used as masking reagents of Cu(II) ions in that range of pH and this make them available for different applications [17–20].

4.2.7 Thermogravimetric Analysis

The thermal behavior of the prepared complexes under investigation was assessed using TGA under N_2 atmosphere. The reported Cu(II) complexes were found to be air stable and have higher thermal stability. The TGA data for the synthesized complexes are summarized in Table 2. Thermal data showed that the lattice water molecules are volatilized within the temperature ranges 24–130 and 31–116 °C for Cunpap and Cunpisnph complexes, respectively. The coordinated water molecules are removed in the temperature ranges 27–207 and 120–215 °C. Finally the complexes undergo decomposition of the organic ligands within the temperature range up to 749 °C, leading to the formation of the copper metallic as final products.

4.2.8 Kinetic Data

The kinetic parameters are listed in Table 2. From the obtained results, the values of ΔG^* increased for the subsequently decomposition stages due to increasing ($T\Delta S^*$) form one stage to another due to the structural rigidity of the remaining complex after expulsion of one and more ligand as compared with the precedent complex, which require more energy [58]. The ΔS^*values for all complexes were found to be negative denoting that the activated complex is more ordered than the reactants and the decomposition reaction is slow [59].

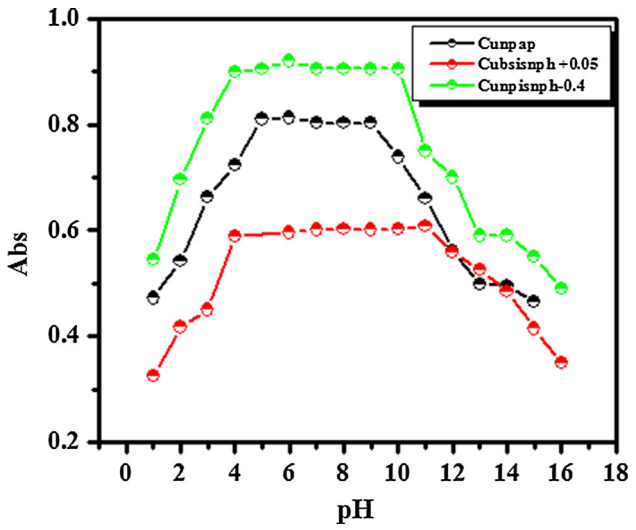

Fig. 5 pH-profile of the prepared complexes in DMF as solvent, at [Cunpap] = [Cubsisnph] = 10^{-3} M and [Cunpisnph] = 5 × 10^{-4} M and 298 K

4.2.9 Particle Size Measurements

TEM images of the Cunpap, Cubsisnph and Cunpisnph complexes are depicted in Fig. 6. The data imply that the Cunpap, Cubsisnph and Cunpisnph complexes have similar morphology of non-uniform nanoparticle shape with average particle size of 40, 50 and 20 nm (as seen in the histograms presented in Fig. 6a, b, c), respectively. These results indicate that the prepared complexes have a high surface area and this can lead to many interesting catalytic and potential properties [60, 61].

4.2.10 Molecular Orbital Calculations

From the elemental analysis and spectroscopic data, Cu(II) metal ion in Cubsisnph was expected to be coordinated to the ligand in its anion form through a nitrogen atom (N22) and oxygen atom (O31) forming six member ring, through a nitrogen atom (N22) and nitrogen atom (N5) forming five member ring and through a nitrogen atom (N5) and oxygen atom (O11) forming five member ring (cf. Figure 7a). In Cubsisnph complex, Cu(II) were expected to be coordinated to the ligand through a nitrogen atom (N1) and oxygen atom (O9) forming sex member ring, through a nitrogen atom (N1) and nitrogen atom (N10) forming five member ring and through a nitrogen atom (N10) and oxygen atom (O13) forming five member ring(cf. Figure 7b).

4.2.10.1 Geometric Parameters of the Prepared Ligands

The values of the structural parameters of the optimized geometry obtained from DFT-B3LYP/6-31G ++(d, p) calculations are informative. The calculated net charges on active centers (cf. Table S6) indicate that the most negative centers are O11, O31, N5 and N22. The donating power as indicating from E_{HOMO} of the anion form is greater than the neutral ligand and the reactivity as indicating from the energy gap of the ligand in its anion form is greater than the neutral ligand by 41 kcal. The non-planarity of the ligand is nicely reflected by the calculated dihedral angles C30C25C23N22, 162°, C23N22C4C37,-48° AND C2C3N5C6, 38°. The values of the dihedral angles indicate that the four centers are not in the same plane. Therefore, the four centers O11, O13, N5 and 22 of the ligand in its

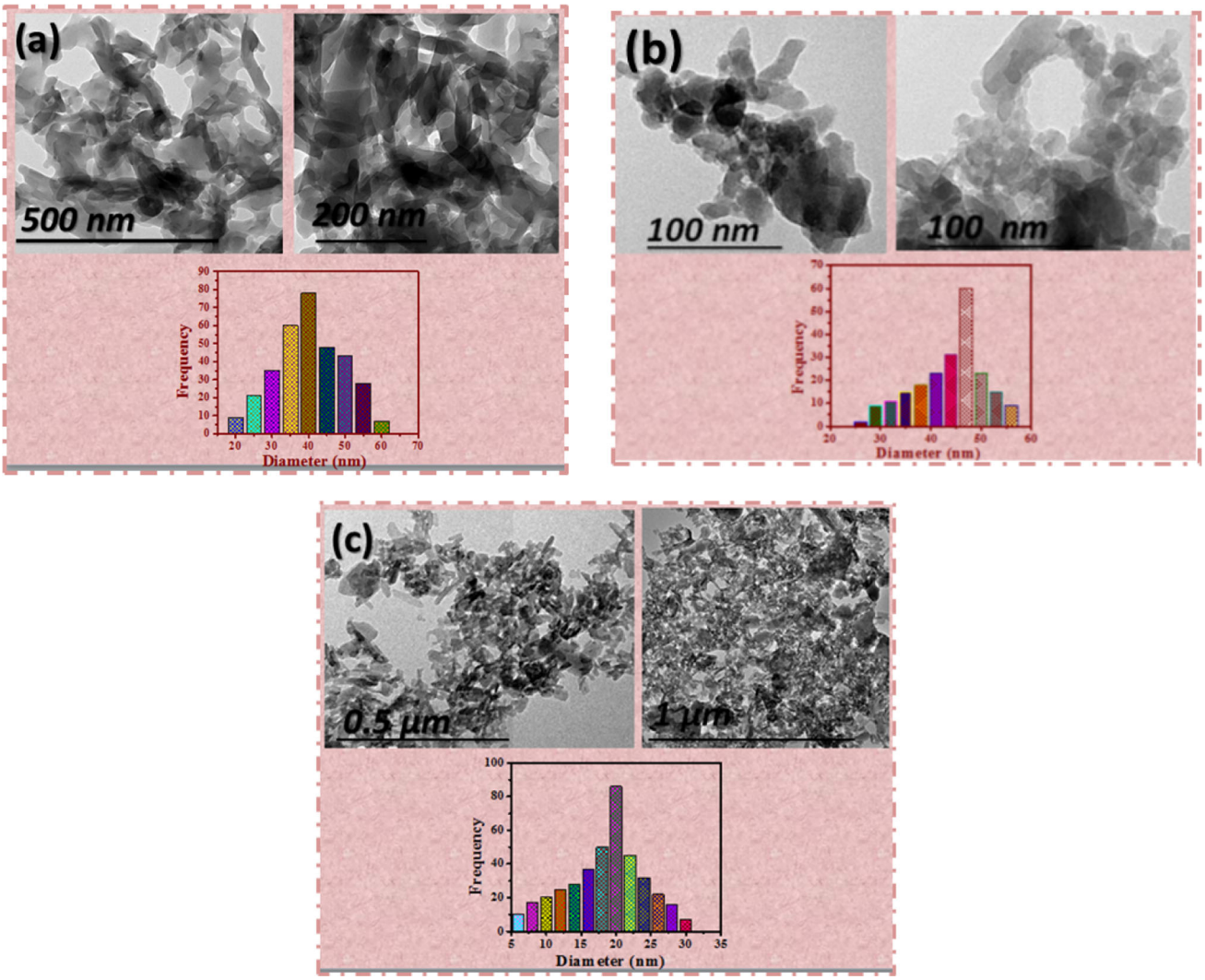

Fig. 6 TEM images and calculated histograms for particle size distribution of the prepared complexes, where **a–c** are for Cunpap, Cubsisnph and Cunpisnph complexes

optimized geometry cannot act as tetradentate ligand to a metal ion. However, M-L complexes studied in this work are well known, well identified and have pronounced activity. The steric effects existing in the ligand force the different fragments to rotate about real single bonds. The ligand is highly labile and the switch-off the molecule from a configuration to the other is facile and takes place in a time of bond formation. Therefore, the four centers O11, O13, N5 and N22 act as tetradentate ligand to a metal ion.

The optimized structure of the npisnph ligand (anion), numbering system and the vector of the dipole moment are presented in Fig. 7b. The energy of the highest occupied MO, E_{HOMO}, energy of the lowest unoccupied MO, E_{LUMO}, energy gap, E_g and the dipole moment computed by B3LYP/6-311G** for the neutral ligand and its anion are presented in Table S6. In addition, the computed geometric parameters were compared with the corresponding values obtained from the experimental data. The optimized bond length of C–C in phenyl rings of (npisnph) ligand fall in the range of 1.37 to 1.425 Å which are greater than the experimentally reported value 1.339 Å, for the C-O bond, the optimized length 1.236 Å is slightly shorter than the experimental value 1.243 Å and the optimized C-N bonds of the ring fall in the range of 1.397 Å to 1.399 Å which are shorter than the experimental value 1.344 Å [62]. The bond angles for DFT-B3LYP/6-311G** reported are slightly better than the HF-method compared to the experimental results. The computation under estimate the < NCC and < OCO angles. The ligand and its anion are non-planer structure with napthyl and indolin-2one moieties are out of the molecular plane of the 5-nitrophenyl ring by 55°. The differences between calculated and measured values can be explained by the fact that the calculations assume an isolated molecule where the

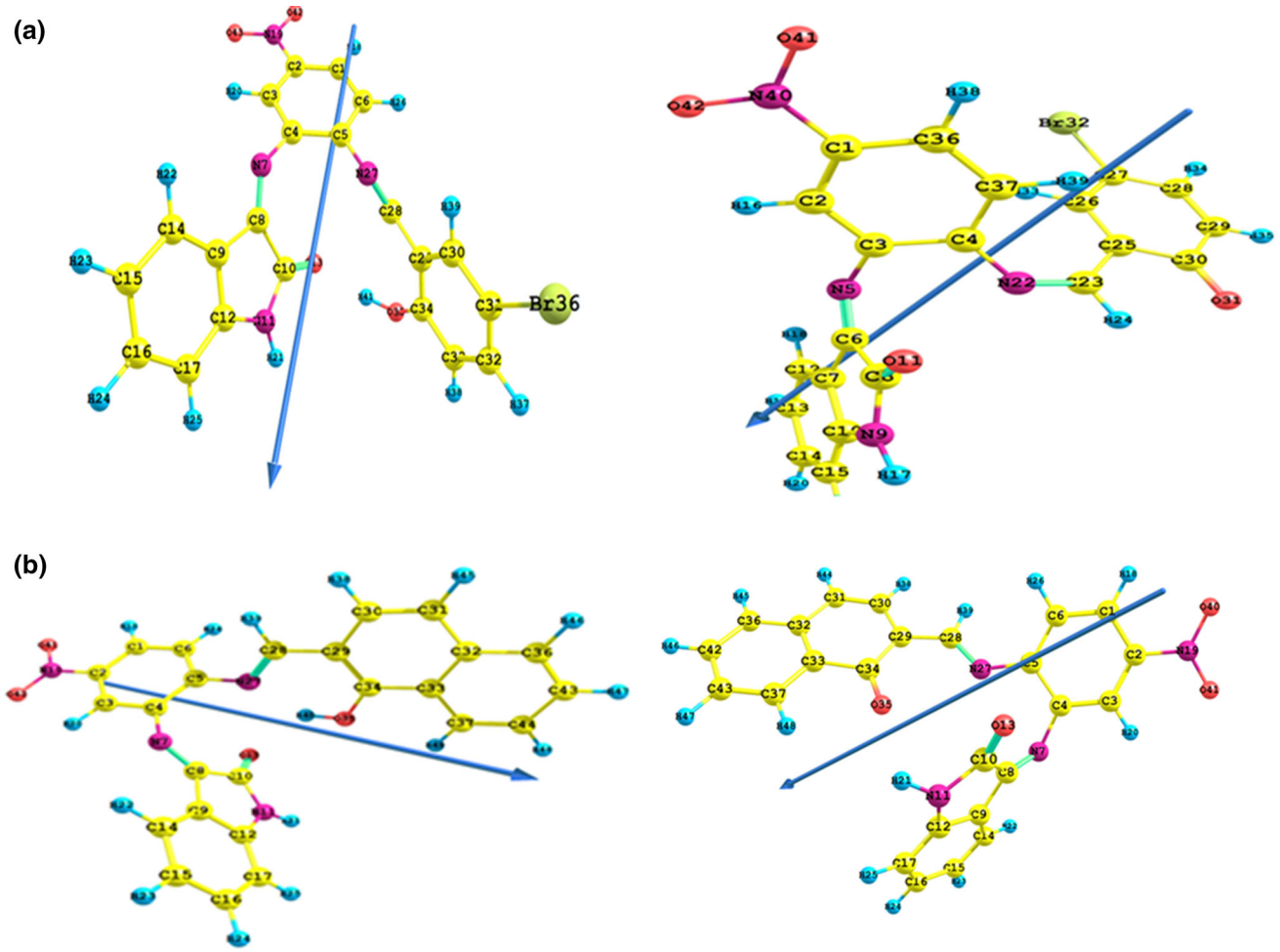

Fig. 7 **a** Optimized geometry numbering system and the vector of the dipole moment for bsisnph Schiff base ligand anion using B3LYP/6-31G**. **b** Optimized geometry numbering system and the vector of the dipole moment for npisnph ligand and its anion using B3LYP/6-31G**

intermolecular columbic interaction with the neighboring molecules are absent, where the experimental results correspond to interacting molecules in the crystal lattice for a similar compound. The ligand npisnph in its anion form is considered as the most electron donor as indicated from computed E_{HOMO} (cf. Table S6). The computed energy gap, E_g, which measure the reactivity shows that npisnph in its anion form is the most reactive ligand (smallest value). The computed dipole moment shows that the anion form of the ligand is less polar than the neutral form by 1.33D (cf. cf. Table S4). From the computed net charge on active centers of the ligand, npisnph in its anion form, it is found that the most negative centers are N27, O35, N7 and O13 which are the centers chelated with the metal to form the complex.

4.2.10.2 Geometric Parameters of the Prepared Complexes Tables S5, S6, S7, S8 and Fig. 8a, b present the optimized geometry, numbering system, the vector of the dipole moment, the energetic, dipole moment, energy gap, net charges on active centers, bond lengths, bond angles and dihedral angles of all metal complexes studied in this work. The electronic configuration for Cu(II) is $3d^9$. In all complexes, metal ion coordinates with O2 and O10 to form six-member ring with N2 and N11 to form five-member ring and with N11 and O14 to form five-member ring. Therefore, distortion from regular octahedral geometry is expected for all the studied complexes. The geometric changes that are noticed in the ligand moiety itself are interesting. Thus, most of bonds show elongation upon complexation with the metal ion. The length of the coordinate covalent bonds between M and the ligand site i.e. M–N and M–O are too long (cf. Table S5), compared to the typical M–X(X = N and O) bond lengths which have the values Cu–O 1.62 Å and Cu–N 1.66 Å [62]. The too long M–O and M–N bonds in the copper complexes mean that

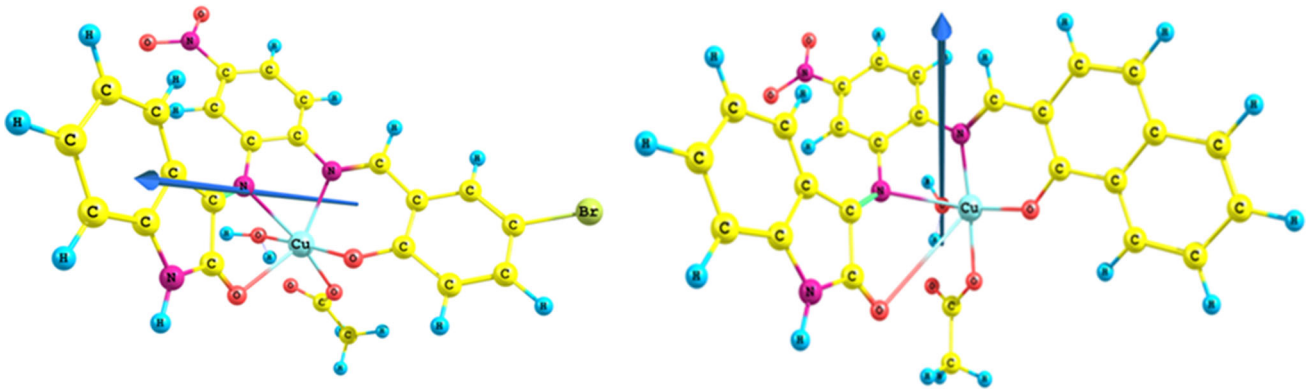

Fig. 8 Optimized geometry, numbering system and the vector of the dipole moment for Cubsisnph and Cunpisnph complexes using B3LYP/LANL2DZ

the ionic character of these bonds is small. Also, the charge on the metal ion in the complex is much less than 2 in Cu (II), hence, the comparison between the calculated (B3LYP/6-31G ++(d, p)) and the typical M(II)-N and M (II)-O is not very precise.

The calculated values of bond angles in Cubsisnph complex between metal ion and binding sites O10MO14, N2MN11, N11MO14 and N2MO10 vary between 83° and 89° which compare nicely with the experimental data as obtained from X-ray data for O_h Cu-complexes [62], which indicates a distorted octahedral geometry. The values of the dihedral angles around metal ion in Cubsisnph i.e. MO10C9C4, MN2C28C30, MO14C13N14 and MO23N24O25 (cf. Table S5) are far from 0.0° or 180° which indicate that the metal ion is not in the same plane of the donating sites. In Cunpisnph complex, the calculated values of bond angles (between metal ion and binding sites) (cf. Table S5) O9MN1, N1MO25, O25MN10, N10MO13 and O13MO21 vary between 85° and 132° which compare nicely with the experimental data as obtained from X-ray data for O_h Cu-complexes [62], which articulates a distorted octahedral geometry.

4.2.10.3 Charge Distribution Analysis In the Cubsisnph and Cunpisnph complexes Cu metal ions ends up with a net charge of 0.5680e and 0.6772e indicating that the two metal ions received 1.4438e and 1.3228e from its surrounding ligand, respectively. The amount of the electronic charge received by each metal ion in the studied complexes is presented in Table S6. There is no electron back–donation from the metal ion to the donating sites (O10, O14, N2 and N11). These results are further confirmed by comparing the values of the calculated charge density on the ligating atoms, in the complex and on the same atoms in the free ligand.

5 Catalytic Activity

5.1 Oxidation of Benzyl Alcohol

The catalytic oxidation of benzyl alcohol in acetonitrile and in some solvents was carried out with Cu(II) Schiff base complexes by using an aqueous H_2O_2 as oxidant (Tables 3, 4, 5) in varies conditions. The catalytic potentiality of benzyl alcohol oxidation is quantitative and good/moderately selective to the corresponding benzaldehyde product with Cunpap complex with some other side products.

5.2 Temperature Effect

To evaluate and optimize the catalytic potentials of Cunpap, Cubsisnph and Cunpisnph complexes (0.05 mmol) towards oxidation of benzyl alcohol (1.00 mmol) as model substrate using an aqueous H_2O_2 as the oxygen source (4.0 mmol) at various temperatures (50, 60, 70, 80 and 90 °C) and for different times in acetonitrile were investigated and collected in Tables 3, 4 and 5 and presented in Fig. 9a–c. The corresponding carbonyl benzaldehyde (BA) thus obtained was analyzed by GC is the target product of the benzyl alcohol oxidation. Control experiments showed that no carbonyl product was formed in a measurable extent in the absence of any catalyst (Cunpap, Cubsisnph or Cunpisnph) in all varies conditions.

Table 3 collects the conversion percentage and chemoselectivity of the oxidation of benzyl alcohol catalyzed by Cunpap complex using an aqueous H_2O_2 solution in acetonitrile at 50, 60, 70, 80 and 90 °C in various times which presented in Fig. 9a. At 50 °C, however, the conversion of the reactant, benzyl alcohol (R) to the target product, benzaldehyde (BA), was the lowest

Table 3 Oxidation of benzyl alcohol catalyzed by Cunpap using an aqueous H_2O_2 in acetonitrile

Entry[a]	Temp. (°C)	Time (h)	Yield (%)[b]				Conversion (%)	Selectivity (%)	TON[d]	TOF[e]
			BA[b]	BZ[c]	Side products	R[a]				
1	50	0.5	46	0	–	54	46	100	9.20	18.40
2		1	48	0	–	52	48	100	9.60	9.60
3		2	46	0	–	54	46	100	9.20	4.60
4		4	40	20	–	40	60	67	12.00	3.00
6	60	0.5	42	0	–	55	42	100	8.40	16.80
7		1	45	20	–	35	65	70	13.00	13.00
8		2	44	23	–	33	67	66	13.40	6.70
9		4	38	30	–	32	68	56	13.60	3.40
10	70	0.5	55	0	–	45	55	100	11.00	22.00
11		1	55	0	12	33	67	82	13.40	13.40
12		2	54	0	15	31	69	78	10.80	5.40
13		4	49	0	16	35	65	75	13.00	3.25
14		6	48	0	18	34	66	73	13.20	2.20
15	80	0.5	40	0	9	51	49	82	9.80	19.60
16		1	44	0	12	44	56	79	11.20	11.20
17		2	46	0	22	32	68	68	13.6	6.80
18		4	38	0	30	36	68	56	13.6	3.40
19	90	0.5	44	0	–	53	44	100	8.80	17.60
20		1	44	–	10	46	54	81	10.80	10.80
21		2	30	37	8	25	75	40	15.00	7.50
22		4	29	33	15	32	77	38	15.40	3.85

[a] The oxidation of benzyl alcohol (R) (1.0 mmol) catalyzed by Cunpap complex (0.05 mmol) with aqueous H_2O_2 (4.00 mmol) in 10 cm^3 acetonitrile for 6 h

[b] The yield based on GC results, selectivity percentage of the target oxide product, benzaldehyde (BA) and the other product, benzoic acid (BZ)

[c] The other side products are mainly of benzoic acid

[d] TON (turnover number) = ratio of moles of product (here oxide) obtained to the moles of catalyst

[e] The corresponding TOF (turnover frequency) (TON/h) are shown in parentheses (mol (mol catalyst)$^{-1}$ h^{-1})

(entry 3, 46 % after 2 h) with no detection of other products by GC. On the other hand, the chemoselectivity of BA percentage was excellent (100 %) as observed in entries 1–3. At higher reaction temperature, 60 °C, the chemoselectivity was improved remarkably in the same conditions (Table 3, entries 6–9) to be 42 % after half hour as a good yield of benzaldehyde percentage (entry 6) with no observation of the presence of benzoic acid (BZ) as a further oxidized product or other side unknown products. With prolongation of the reaction time, the amount of BA was reduced by time from 45 to 38 % with increasing of benzoic acid and other unknown side products percentages (entries 7–9). In another words, after half hour, a further oxidation of the target product, BA, took place to afford BZ with increasing of conversion and decreasing of its chemoselectivity. At 70 °C, both of the chemoselectivity and the conversion was little improved and progressed remarkably up to 55 % of BA after half hour without presence of an observed other unknown side products and reactant percentage as detected by GC (entry 10). After 6 h of the reaction, the yield of the chemoselective product, BA has not been improved but reduced to 48 % in absence of any amount of BZ and an observable amount of unknown other side products and reactant, 18 and 34 % respectively (entry 14). At 80 °C, the chemoselectivity and the conversion was reduced to awarded moderate yield of BA, 44 % (entry 16) with very low percentage of other side products (12 %). Moreover, at 90 °C, similar behavior in the catalytic process was observed affording good yield of BA (44 %) after one hour (entry 20). Consequently, the optimized conditions for the catalytic potential of Cunpap complex (0.05 mmol) as a catalyst for the oxidation of benzyl alcohol in acetonitrile using an aqueous H_2O_2 as a terminal oxidant are at 70 °C and after half hour (entry 10), Fig. 9a, as detected by GC.

Similarly, for Cubsisnph complex, Table 4 shows the effect of temperature on the oxidation of benzyl alcohol

Table 4 Oxidation of benzyl alcohol catalyzed by Cubsisnph complex using an aqueous H_2O_2 in acetonitrile

Entry[a]	Temp. (°C)	Time (h)	Yield (%)[b]				Conversion (%)	Selectivity (%)	TON[d]	TOF[e]
			BA[a]	BZ[b]	Side products	R				
1	50	0.5	38	–	–	62	38	100	7.60	15.20
2		1	47	–	–	53	47	100	9.40	9.40
3		2	38	11	–	51	49	78	9.80	4.90
4		4	36	25	–	39	61	59	12.20	3.05
5		6	22	40	–	38	62	35	12.40	2.07
6	60	0.5	62	–	–	38	62	100	12.4	24.8
7		1	90	–	–	10	90	100	18	18
8		2	57	43	–	–	100	57	20	10
9		4	30	52	–	18	82	37	16.40	4.10
10		6	21	53	–	26	74	28	14.8	2.47
11		8	14	55	17	24	86	16	17.20	2.15
12	70	0.5	54	–	–	46	54	100	10.80	21.60
13		1	40	25	–	35	65	62	13.00	13.00
14		2	36	36	–	28	72	50	14.40	7.20
15		4	29	42	–	29	71	42	14.20	3.55
16		6	18	55	–	27	73	25	14.60	2.43
17	80	0.5	36	29	–	35	65	55	13.00	26.00
18		1	33	32	4	31	69	48	13.80	13.80
19		2	20	34	18	28	72	28	14.40	7.20
20		4	6	44	27	23	77	8	15.40	3.85
21	90	0.5	0	75	25	0	100	0	–	–
22		1	–	70	30	0	100	0	–	

[a] The oxidation of benzyl alcohol (R) (1.0 mmol) catalyzed by Cubsisnph complex (0.05 mmol) with aqueous H_2O_2 (4.00 mmol) in 10 cm^3 acetonitrile for 6 h

[b] The yield based on GC results, selectivity percentage of the target oxide product, benzaldehyde (BA) and the other product, benzoic acid (BZ)

[c] The other side products are mainly of benzoic

[d] TON (turnover number) = ratio of moles of product (here oxide) obtained to the moles of catalyst

[e] The corresponding TOF (turnover frequency) (TON/h) are shown in parentheses (mol (mol catalyst)$^{-1}$ h^{-1})

oxidized by H_2O_2 at 50, 60, 70, 80 and 90 °C and presented in Fig. 9b. At low temperature, 50 °C, the catalytic process show slow reactivity with low percentage of the target product (38–22 %) with high to moderate residual amount of the reactant from 0.5 to 6 h (Table 4, entries 1–5), respectively. However, some amounts of benzoic acid, BZ percentages appeared after 3, 4 and 6 h (11, 25 and 40 %, entries 3, 4 and 5 respectively) with maximum chemoselectivity at 50 °C after 1 h is 47 %.

When the temperature increased to 60 °C in the same conditions, there some improvement for the yield percentage of BA percentage after 1 h (as the optimized reaction conditions) to afford 90 % with no detection of other side products (entry 7), this means that the conversion is 90 % and the selectivity is 100 %. Nevertheless, by running the catalytic process for longer time (entry 8), the selectivity dropped down little bit to be 57 % with the same conversion percentage of benzyl alcohol, i.e., formation of benzoic acid BZ 43 %. After longer time in the same temperature, it seems that the selective product underwent further oxidation from BA to BZ and the other side products with reducing of the chemoselectivity (entries 9, 10 and 11 with selectivity 37, 28 and 18 % of BA after 4, 6 and 8 h respectively). By improving the reaction temperature to 70 °C, after half hour, the residual of the reactant was 46 % with high selectivity and conversion of BA (100 and 54 %, respectively, entry 12). Furthermore, after l hour, the selectivity reduced (40 % of BA) with improving of the conversion (with other side product, BZ, 25 %, entry 13). Prolongation of time, as shown in Table 4, entries 14–16, the selectivity percentages of the oxidation process reduced remarkably to afford improvement of BZ percentages in the catalytic process (36, 42 and 55 %, entries 14, 15 and 16 respectively) with an observable increase in the

Table 5 Oxidation of benzyl alcohol catalyzed by Cunpisnph complex using an aqueous H_2O_2 in acetonitrile

Entry[a]	Temp. (°C)	Time (h)	Yield (%)[b]				Conversion (%)	Selectivity (%)	TON[d]	TOF[e]
			BA[a]	BZ[b]	Side products	R				
1	50	0.5	24	–	–	76	24	100	4.80	9.60
2		1	24	23	–	53	47	51	9.40	9.40
3		2	32	21	–	47	53	60	10.60	5.30
4		4	32	23	–	45	55	58	11.00	2.75
5		6	32	34	–	34	66	49	13.20	2.20
6		8	21	42	–	37	63	33	12.60	1.58
7	60	0.5	42	17	–	41	59	72	11.80	23.60
8		1	79	–	–	21	79	100	15.80	15.800
9		2	47	25	–	28	72	65	14.40	7.20
10		4	44	30	–	26	74	59	14.80	3.70
11	70	0.5	26	0	–	74	26	100	5.20	10.40
12		1	55	0	–	45	55	100	11.00	11.00
13		2	55	0	–	45	55	100	11.00	5.50
14		4	45	19	–	36	64	70	12.80	3.20
15		6	44	31	–	25	75	59	15.00	2.50
16	80	0.5	29	29	–	42	58	50	11.60	23.20
17		1	43	26	–	31	69	62	13.80	13.80
18		2	28	33	–	29	61	46	12.20	6.10
19		4	41	43	–	26	84	49	16.80	4.20
20	90	0.5	43	21	–	36	64	67	12.80	25.60
21		1	–	100	–	0	100	–	20.00	20.00

[a] The oxidation of benzyl alcohol (R) (1.0 mmol) catalyzed by Cunpisnph complex (0.05 mmol) with aqueous H_2O_2 (4.00 mmol) in 10 cm^3 acetonitrile for 6 h

[b] The yield based on GC results, selectivity percentage of the target oxide product, benzaldehyde (BA) and the other product, benzoic acid (BZ)

[c] The other side products are mainly of benzoic acid

[d] TON (turnover number) = ratio of moles of product (here oxide) obtained to the moles of catalyst

[e] The corresponding TOF (turnover frequency) (TON/h) are shown in parentheses (mol (mol catalyst)$^{-1}$ h^{-1})

conversion. Similar behavior took place of the catalytic oxidation of benzyl alcohol at 80 °C. The selectivity percentage was in moderate at longer time with increase of the conversion percentage by time (36, 33, 20 and 6 %, entries 17–20, respectively). At very high reaction temperature, 90 °C, most of the reaction components evaporated and the evaluation of the component percentages were difficult and have high error in GC. However, the results obtained in Table 4 (entries 21 and 22) show that there was no detection of the selective product (BA) in the reaction media. Consequently, the catalytic potentiality of benzyl alcohol oxidation is quantitative and highly selective to the corresponding carbonyl product with Cubsisnph with some other side products. It seems that Cubsisnph complex as a catalyst has more catalytic activity for oxidation of benzyl alcohol to the chemoselective product (benzaldehyde) than Cunpap complex (Table 4, entry 7, Table 3, entry 10, respectively). Cubsisnph complex afforded at optimized conditions (at 60 °C and after 1 h) conversion 90 % of the target product (BA) with no detection of BZ or other side products with chemoselectivity 100 %, Fig. 9b.

From Table 5 and Fig. 9c, the catalytic potential of Cunpisnph complex for oxidation of benzyl alcohol to the chemoselective product benzaldehyde is very similar to that of both Cunpap and Cubsisnph complexes (Table 3 entry 7, Table 4, entry 10, respectively), but Cubsisnph complex is more reactive than Cunpisnph complex. Table 5 shows the effect of temperature on the catalytic oxidation of benzyl alcohol to the chemoselective product, benzaldehyde, using Cunpisnph complex as a catalyst, in which the reaction was repeated in typical conditions at 50, 60, 70, 80 and 90 °C, as for Cunpap and Cubsisnph complexes. At low temperature (50 °C), the catalytic potential of Cunpisnph complex is low for all catalytic runs from half hour to s6 h (entries 1–6) which has similar behavior as Cunpap and Cubsisnph complexes. The chemoselective

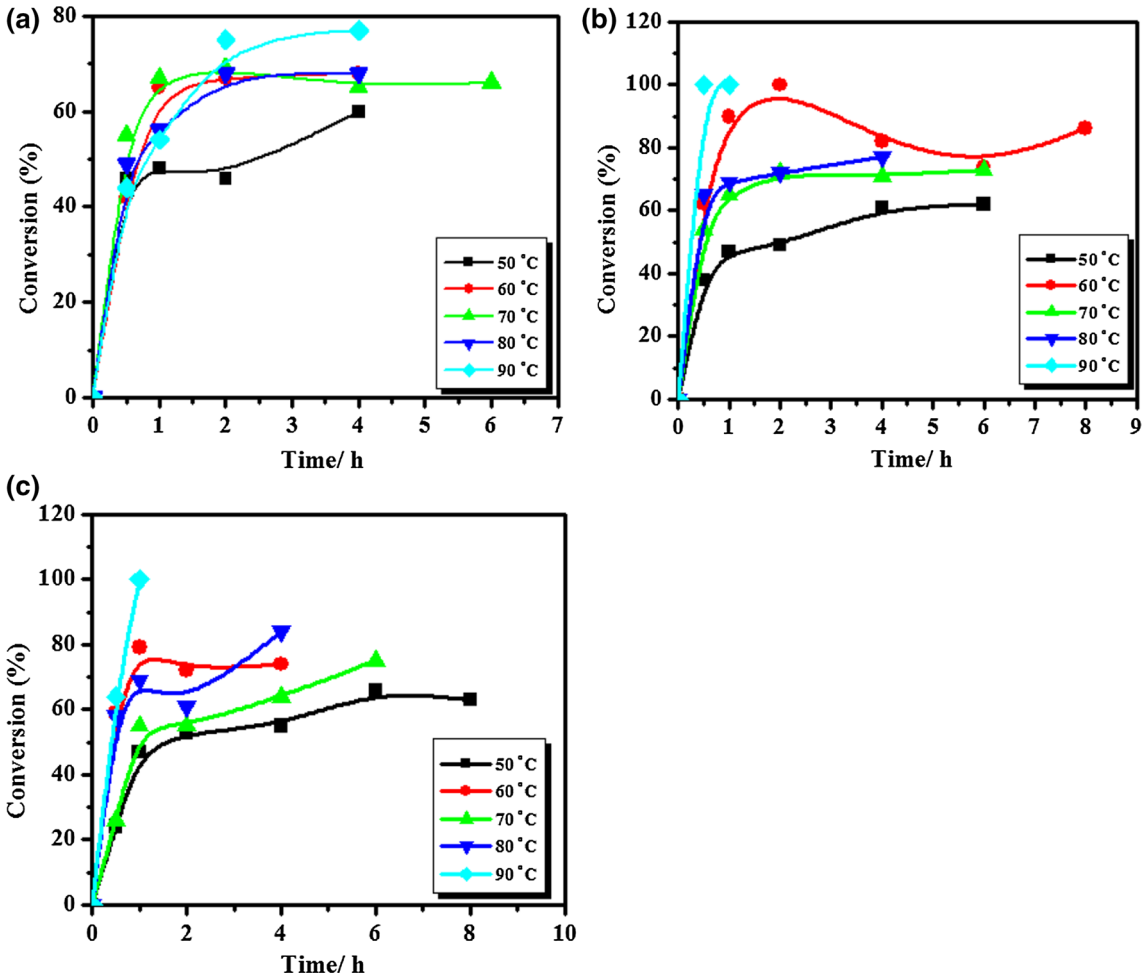

Fig. 9 **a** Influence of temperature on benzyl alcohol oxidation by Cunpap complex. **b** Influence of temperature on benzyl alcohol oxidation by Cubsisnph complex. **c** Influence of temperature on benzyl alcohol oxidation by Cunpisnph complex

product percentage has been improved by time from 24 % after half hour to 32 % after 6 h, in which the amount of benzoic acid increased from zero after half hour to 34 % after 6 h (entries 1- 5). At the end, after 8 h, the amount of the target product was reduced to 21 % with increase of benzoic acid content to be 42 % (Table 5, entry 6). Consequently, the chemoselectivity at 50 °C by the time increased till 6 h with improvement of the conversion but after long time (8 h) the selectivity reduced (21 %) with high increase of the conversion to be (63 %) with no observed formed other unknown side products as detected by GC. At 60 °C, the chemoselectivity was improved to moderate after half hour (42 %), but after 1 h, it was good to afford 79 % of the target product with no amount of benzoic acid or other side unknown products. This result shows that the optimized catalytic reaction conditions are at 60 °C for 1 h to afford good yield of benzaldehyde (Table 4, entry 8). The conversion and the chemoselectivity are good to 79 %. At higher temperature (70 and 80 °C) the catalytic potential of Cunpisnph complex was reduced and did not afford better yield of the chemoselective product BA (Table 5, entries 11–20). This behavior of Cunpisnph complex is very close to that of Cubsisnph complex. At very high reaction temperature, 90 °C, similarly, most of the reaction components were evaporated, however, entry 20 presented good yield of BA after half hour. Nevertheless, after one hour the reaction conversion was directed to BZ only with no detection of BA or other side unknown products (entry 21).

Conclusively, Cunbisnph complex has more catalytic activity for the benzyl alcohol oxidation to the chemoselective product, benzaldehyde, than Cunpap and Cunpisnph complexes (Table 3, entry 10, Table 4, entry 6, and Table 5, entry 8, respectively) at the optimized reaction conditions (after 1 h at 60 °C for Cunbisnph and Cunpisnph and 0.5 h at 70 °C for Cunpap in acetonitrile).

5.3 Effect of Catalyst Type

Oxidation of benzyl alcohol by an aqueous H_2O_2 solution catalyzed by Cunpap, Cubsisnph or Cunpisnph complex in acetonitrile at the optimum conditions awarded moderate to high yield of the chemoselective reaction product (BA), Tables 3, 4 and 5 (Fig. 9a–c). However, there is no remarkably change in the catalytic activity between the current catalysts, however, Cunbisnph complex is most reactive catalyst (90 % of BA after 1 h). Cunpisnph complex has lower reactivity by 79 % of BA after one hour and Cunpap complex has the lowest catalytic reactivity by 55 % of BA after half hour. The solubility and polarity of the studied catalyst complexes may play a major role in acetonitrile, Cunpap complex is the less soluble and polar catalyst, in the other hand, Cubsisnph and Cunpisnph complexes are more polar and soluble in acetonitrile. This could be explained due to the presence of acetate group as coordinated ligand, which increases the polarity of the catalyst complexes (cf. Scheme 1) in Cubsisnph and Cunpisnph complexes. Furthermore, in Cunpap complex, copper ion surrounded by two coordinated Schiff base ligands, which may block the active sides of Cu^{2+} ions for catalysis [63]. In addition, the presence of coordinated water molecules in Cubsisnph and Cunpisnph complexes may improve their catalytic potentials towards benzyl alcohol oxidation by an aqueous H_2O_2. This behavior of the catalyst complexes will be discussed in details in the mechanism later.

5.4 Effect of Solvent

The catalytic potential of the current Cu(II) complex catalysts (0.05 mmol) towards oxidation of benzyl alcohol (1.0 mmol) by an aqueous H_2O_2 (4.0 mmol) in different solvents (acetonitrile, N,N′-dimethylformamide (DMF), acetone, dichloromethane carbon tetrachloride and chloroform) is studied and collected in Table 6. All catalytic processes were carried out in the optimized conditions for all complex catalysts, as reported in Tables 3, 4 and 5. From Table 3, the catalytic activity has been remarkable influenced by the nature of the solvent on benzyl alcohol oxidation, as reported previously [64]. For Cunpap complex, the results illustrate the conversion control and chemoselectivity percentage of benzyl alcohol oxidation at 70 °C after half hour in various solvents with trend of the catalytic potentials was ordered as: in acetonitrile > acetone > dichloromethane > chloroform > DMF. The highest conversion percentages were obtained in acetonitrile (55 %), whereas, in all other solvent, the chemoselectivity to the target product percentages were low. The catalytic potentials of Cubsisnph and Cunpisnph complexes are very close to the pervious Cunpap complex in those solvents (Table 6). Both gave low reactivity toward oxidation of benzyl alcohol using an aqueous H_2O_2 in their optimized conditions to BA with different conversion rates (at 70 °C after one hour or half hour for at 60 °C Cubsisnph or Cunpisnph complexes respectively) in all solvents other than acetonitrile.

The polarity of the various solvents in the catalytic oxidation of alcohols is playing a major role for the stereo- and chemoselectivity, and conversion percentages. Only in acetone the catalytic process was little more reactive for the conversion and chemoselectivity to BA for all catalyst complexes (e.g., 58 % selectivity with 31 % conversion, using Cunpap complex). It seems that in aprotic solvents, i.e. acetonitrile, a good oxidation chemoselective product is observed using our studied catalysts, as also observed in in the lowest dielectric constants solvents, i.e. dichloromethane, in which the oxidation conversion is very good (100 % with all catalysts) but with moderate to high chemoselectivity (Table 6). This means that, the target product percentage is 17, 1 or 1 % using Cunpap, Cubsisnph or Cunpisnph complexes respectively. DMF is known as a highly coordinated solvent, which may activate strongly the catalyst for the oxidation of benzyl alcohol but with no conversion control and no chemoselectivity to the target product with all catalysts (almost zero percentage of BA), (cf. Table 6). Interestingly, the very close observed amount of the product of benzaldehyde was observed by GC in those solvent using either Cubsisnph or Cunpisnph complex as a catalyst in the oxidation of benzyl alcohol could be explained in the term of chemical structure of both Cubsisnph and Cupsisnph complexes. Conclusively, the most effective and suffusion solvent for the catalytic oxidation of benzyl alcohol using H_2O_2 catalyzed by Cunpap, Cubsisnph and Cunpisnph complexes is acetonitrile as observed previously [65].

5.5 Effect of Catalyst Amount

The amount of the catalysts for the oxidation processes of primary alcohols, e.g. benzyl alcohol, have an interesting feature and impact on the amount of the reaction kinetics and yield of the corresponding carbonyl products, e.g. benzaldehyde, as remarked before for the oxidation processes [63]. The effect of the catalyst was discovered by insertion of different molar ratios of the Cunpap complex to benzyl alcohol in the oxidation process (0.02, 0.05 or 0.10: 1, respectively) using an aqueous H_2O_2 in acetonitrile at optimized conditions. The results are presented in Table 7. It seems that, by increasing of the catalyst molar ratios from 0.02 to 0.10 mmol, the catalytic potential of Cunpap complex was improved. With 0.02 mmol of Cunpap complex, the percentage of the target product was zero with 53 % of other side products, in another words, the

Table 6 Effect of solvent on catalytic activity of benzyl alcohol

Complex	Solvent							
	$CHCl_3$		CH_3COCH_3		CH_2Cl_2		DMF	
	Conversion (%)	Selectivity (%)	Conversion (%)	Selectivity (%)	Conversion (%)	Selectivity (%)	Conversion (%)	Selectivity (%)
Cunpap	16	31	31	58	100	17	100	0
Cubsisnph	100	4	100	10	100	1	100	0
Cunpisnph	19	100	100	7	100	1	100	1

Table 7 Effect of catalyst concentration on the oxidation of benzyl alcohol with molecular oxygen using copper complexes

Complex	Catalyst concentration (mmol)					
	0.02		0.05		0.1	
	Conversion (%)	Selectivity (%)	Conversion (%)	Selectivity (%)	Conversion (%)	Selectivity (%)
Cunpap	53	–	55	100	100	45
Cubsisnph	100	19	90	100	100	–
Cunpisnph	53	–	79	100	100	45

chemoselectivity was zero and the conversion was 53 %. But, with higher amount of the catalyst in the benzyl alcohol oxidation process (0.02 mmol), the chemoselectivity increased remarkably to be 55 % to the best amount with strong dropping of the side products to be 18 %. With 0.05 mmol of the catalyst complex, the chemoselectivity and conversion was strongly improved. From Table 7, at the highest amount of the Cunpap complex (0.10 mmol), the chemoselectivity increased for the amount of the needed product (benzaldehyde) but not strongly like the catalyst amount 0.05 mmol as observed in Table 7. We concluded that the optimized reaction amount of the Cunpap complex for the oxidation of benzyl alcohol by H_2O_2 in acetonitrile at 70 °C for 1 h is 0.05 mmol. The above results indicate that Cunpap complex is not highly an effective catalyst for the hydrogen peroxide oxidation of alcohols under various reaction conditions.

As repeated step, the effect of Cubsisnph catalyst was discovered by insertion of different molar ratios (0.02, 0.05 or 0.10: 1.00) of the Cubsisnph complex to benzyl alcohol in the oxidation process using an aqueous H_2O_2 in acetonitrile at 60 °C for 1 h. The results are presented in Table 7. It seems that by increasing of the catalyst molar ratios from 0.02 to 0.10 mmol, the catalytic potential of Cubsisnph complex was improved. With 0.02 mmol of Cubsisnph complex, the percentage of the target product was 19 % with no remarked amount of the other side products, i.e., the chemoselectivity was 19 % and the conversion was 100 %. However, with higher amount of the catalyst (0.05 mmol) in the benzyl alcohol oxidation process, the chemoselectivity increased remarkably to be 90 % to the best amount with no remarked amount of the other side products. The chemoselectivity and conversion was strongly improved with 0.05 mmol of the Cubsisnph complex. From Table 7, with 0.10 mmol Cubsisnph complex, the chemoselectivity increased to 45 % of the needed product. We concluded that the optimized reaction amount of the catalyst Cubsisnph complex for the oxidation of benzyl alcohol by H_2O_2 in acetonitrile at 60 °C for 1 h is 0.05 mmol. The above results indicate that Cubsisnph complex is not highly an effective catalyst for the hydrogen peroxide oxidation of alcohols under various reaction conditions. Consequently, the effect of the catalyst was discovered by insertion of different molar ratios of the Cunpisnph complex to benzyl alcohol in the oxidation process (0.02, 0.05 or 0.10: 1, respectively) using aqueous H_2O_2 in acetonitrile at 60 °C for 1 h. The results are presented in Table 7. It seems that by increasing of the catalyst molar ratios from 0.02 to 0.10 mmol, the catalytic potential of Cunpisnph complex improved. With 0.02 mmol of Cunpisnph complex the percentage of the target product was 37 with 53 % of other side products, in another words, the chemoselectivity was zero and the conversion was 90 %. Furthermore, with higher amount of the catalyst in the benzyl alcohol oxidation process (0.05 mmol), the chemoselectivity increased remarkably to be 79 % to the best amount with no observation of the side products. The highest amount of Cunpisnph complex (0.10 mmol), the chemoselectivity increased for the amount of the needed product, benzaldehyde (48 %), but not strongly like the

catalyst amount 0.05 mmol, as observed in Table 5. This behavior is similar to that of Cunpap and Cunbisnph catalysts. We concluded that the optimized reaction amount of Cunpisnph catalyst for the oxidation of benzyl alcohol by H_2O_2 in acetonitrile at 60 °C for 1 h is 0.05 mmol. The above results indicate that Cunpisnph complex is not highly an effective catalyst for the hydrogen peroxide oxidation of alcohols under various reaction conditions.

5.6 Mechanistic Aspects

Benzyl alcohol was subjected to the oxidation protocol under the influence of Cunpap, Cunbisnph and Cunpisnph catalysts using an aqueous H_2O_2 as terminal oxidant, in order to establish the catalytic applicability of the current complex catalysts. Tables 3, 4 and 5 summarized the oxidation product yield of benzyl alcohol by chemoselectivity using an aqueous H_2O_2 in acetonitrile catalyzed by Cunpap, Cunbisnph or Cunpisnph complexes. The catalytic potential of the current complexes might be attributable for their high stability in various solvents, in which the complexes are octahedral structures (cf. Scheme 1). The structural features of the characteristic Cu^{2+} complex unit with various-dentate Schiff base ligands [66, 67] are illustrated in the suggested mechanism. Cunbisnph and Cunpisnph complexes (as tetradentate Schiff base units) have an open coordination site for the oxidant activation occupied by a water molecule or an acetate ion (cf. Scheme 1) which may be useful for catalytic oxidation reactions, whereas, Cunpap complex (bis-tridentate ONN Schiff base units) act as closed and more stable complex catalyst. Cunbisnph and Cunpisnph complexes are little more reactive than Cunpap complex as catalysts for the oxidation of benzyl alcohol using an aqueous H_2O_2 (Tables 3, 4, 5). In another words, oxygen transfer from the oxidizing agent to the catalyst complex would be easier with Cunbisnph and Cunpisnph complexes than with Cunpap complex, as observed previously [68, 69]. Inspections of the results in Tables 3, 4 and 5 indicate several useful features of this catalytic process. The least reactive benzyl alcohol oxidized in desired times in low/-good yields and excellent selectivities with an aqueous H_2O_2 in which the chemoselectivity of the procedure was notable and measured by GC. In Cubsisnph and Cunpisnph complexes (as tetradentate units), the coordinated water molecule or the acetate ion may play a major role for their high catalytic activity compared to that of Cunpap complex. Cubsisnph and Cunpisnph complexes have an open coordination site for the oxidant (H_2O_2) to replace water molecule or acetate ion and could bond directly to the central metal ion, Cu^{2+} (cf. Scheme 1). This causes probably oxidation of Cu^{2+} ion and oxygen transfer from H_2O_2 to Cu^{2+} [68, 69]. This behavior could be detected particularly by very little change in the spectral scan of the characteristic Cubsisnph complex representively before and after addition of H_2O_2 to Cubsisnph complex in acetonitrile at 60 °C (from 420 to 428 nm). The very little change in the electronic spectral scan of Cubsisnph complex could be attributable for the replacing of H_2O by H_2O_2 molecules. This may be more acceptable than the proposed replacing of acetate ion by H_2O_2 molecule (Fig. 10c) in the tentative mechanistic pathway. Obviously, Cunpap complex has no coordinated water molecule or acetate ion (cf. Scheme 1), only bis-tridentate ONN Schiff base units) act as two surrounded closed ligands. This could be the reason that Cunpap catalyst is less reactive than Cubsisnph and Cunpisnph complexes as catalysts for the oxidation of benzyl alcohol using H_2O_2, as shown in Tables 3, 4, 5 and Fig. 9a–c. Hence, within Cunpap catalyst, H_2O_2 molecule highly probably break any of the coordinated O, N, N units, which may the weakest one to coordinate to the central metal ion, i.e. Cu^{2+} ion. This propose could be more rationalized in the mechanism due to the remarkable change in the characteristic electronic spectral scan of Cunpap catalyst before and after addition of H_2O_2 to Cunpap catalyst in acetonitrile, as seen in Fig. 10a, b. In Fig. 10a, there is an observable violet shift in the characteristic absorption band of Cunpap catalyst after addition of H_2O_2 (from 480 to 470 nm). Furthermore, in Fig. 10b, the observed changes of the repeated electronic spectral scans of Cunpap catalyst in the oxidation process of benzyl alcohol by H_2O_2 in acetonitrile may provide that suggestion by coordination of H_2O_2 to Cunpap catalyst and may be followed by oxygen transfer from the coordinated H_2O_2 to the central metal ion Cu^{2+}, as shown below in the mechanistic steps.

Coordination of H_2O_2 to Cunpap or Cubsisnph solution in acetonitrile may provide oxygen transfer from the coordinated H_2O_2 to Cu^{2+} to afford Cu^{2+}=O unit [Scheme 2**(I, II)**] with a remarkable shift of the characteristic absorption maximum wavelength (λ_{max}) of Cunpap or Cubsisnph catalyst (Fig. 10a, c). This behavior has been reported previously [68, 69] and proved particularly by the electronic spectral scan in the reaction media before and after addition of aqueous H_2O_2 (Fig. 10b, d). This little observable shift at the characteristic maximum absorption bands (λ_{max}) may be attributable for the oxidation of central metal ion Cu^{2+} in the Cunpap or Cubsisnph catalyst by the oxygen source, an aqueous H_2O_2 solution, affording Cu^{2+}=O in the reaction media, as shown in [cf. Scheme 2 (**I**, **III**)].

The electronic spectral scan of Cunpap or Cubsisnph complexes in acetonitrile solution before and after adding aqueous H_2O_2 at 60 °C, respectively, at the optimized conditions for the oxidation of benzyl alcohol, indicates that the catalyst is stable under the catalysis conditions

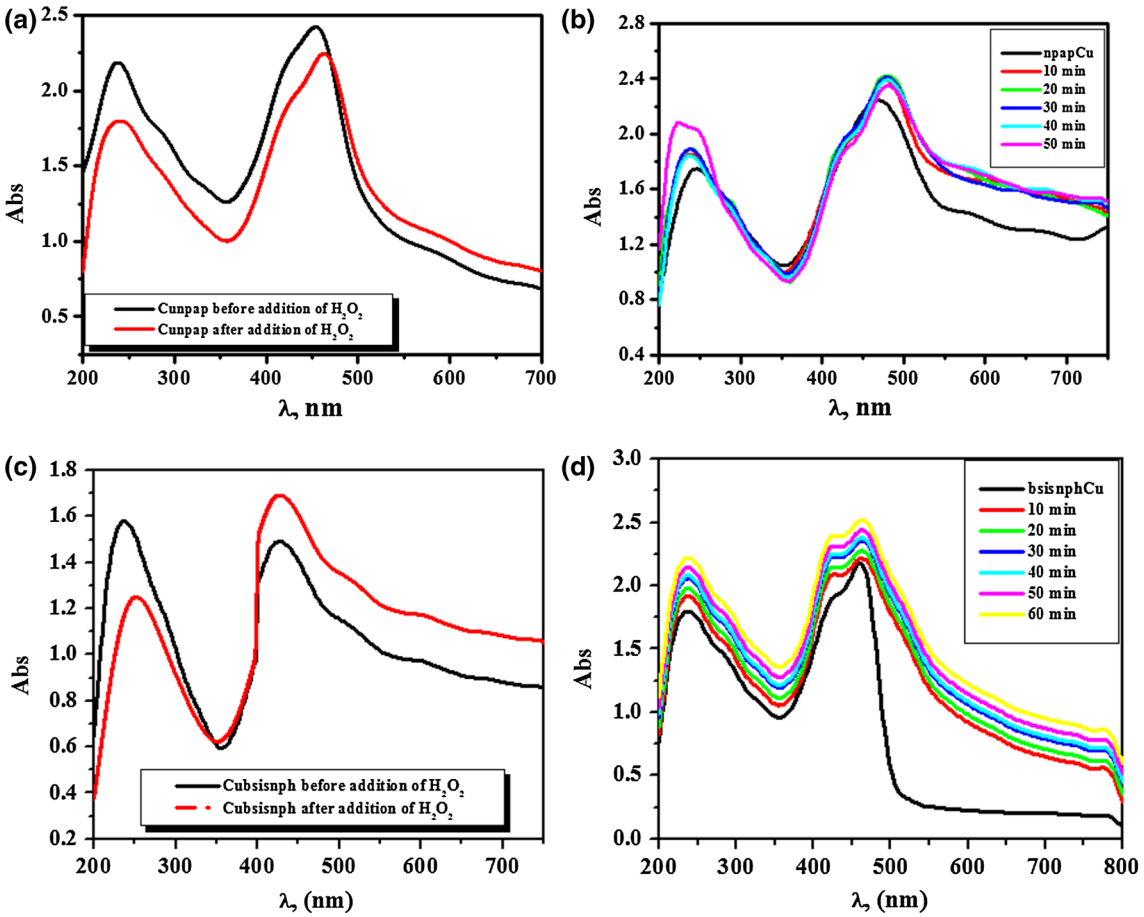

Fig. 10 **a** Electronic spectral scan of Cunpap complex in absence of an aqueous H_2O_2 and in the presence of an aqueous H_2O_2 in acetonitrile at70 °C. **b** Repeated electronic spectral scan of Cunpap complex with benzyl alcohol in the presence of an aqueous H_2O_2 in acetonitrile at 70 °C. **c** Electronic spectral scan of Cubsisnph complex in absence of an aqueous H_2O_2 and in the presence of an aqueous H_2O_2 in acetonitrile at 60 °C. **d** Repeated electronic spectral scan of Cubsisnph complex with benzyl alcohol in the presence of an aqueous H_2O_2 in acetonitrile at 60 °C

(Fig. 10a–d) without any decomposition of the catalyst complexes in the catalytic process. The above observations are in stark contrast with previous reports, where benzyl alcohol oxidation by Cu^{2+} complexes was described for the reaction of Cu^{2+} central ion in the catalyst complex with H_2O_2 as an oxidant to afford the oxide catalyst complex Cu^{2+}=O [68] with extraction of water molecule. By oxygen transfer from the oxidant H_2O_2 molecule in the complex catalyst to afford an activated intermediate, as shown in the mechanistic [cf. Scheme 2(**III**)] resulted water molecule with an active intermediate catalyst complex. The most probability for the stability of Cu^{2+} ions in the reaction media has elucidated by monitoring the repeated electronic spectral scans of complex in the oxidation process (Fig. 10b, d). The intensity of the characteristic absorption bands has approximately little shift during the reaction.

That little shift in the intensity of the characteristic absorption bands (Fig. 10a, c) upon addition of the oxidant and benzyl alcohol is probably due to the formation of active species in the oxidation reaction by coordination of benzyl alcohol to the central metal ion and [cf. Scheme 2(**I, III**)] [68, 69]. According to the designed tentative mechanism, the fourth stage of the process is the formation an active intermediate [cf. Scheme 2(**IV**)] by the combination of the oxidized central metal ion Cu^{2+}=O to the substrate, benzyl alcohol through the oxygen atom of the alcoholic OH group in the benzyl alcohol. This may be proved by the same repeated spectral scan of the complex catalysts after addition of H_2O_2 and benzyl alcohol to the reaction media. In another words, the continuous shift of the characteristic absorption maximum bands of the catalysts (Fig. 10b, d) of Cunpap and Cubsisnph complexes, might be due to the oxidation of the combined benzyl alcohol to the corresponding coordinated aldehyde within extraction of water molecule in the proposed reaction mechanism [cf. Scheme 2(**IV**)], as expected elsewhere [68–71]. This final step in the reaction mechanism involves extraction of the

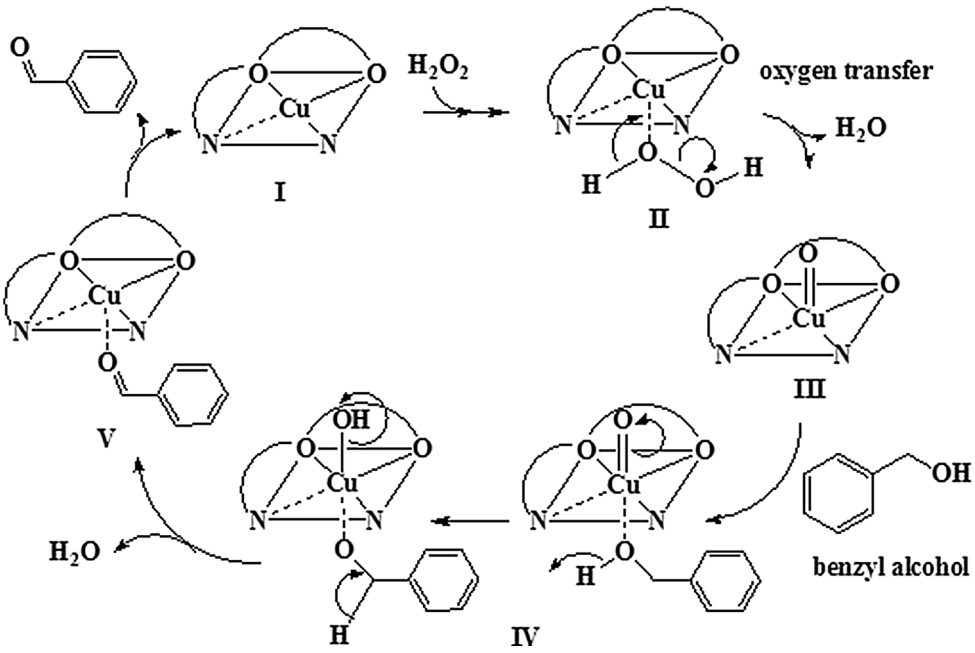

Scheme 2 The tentative mechanism for oxidation of benzyl alcohol catalyzed by the Cu(II)-Schiff base complexes

chemoselective product, benzaldehyde with reduction of the activated catalyst intermediate [cf. Scheme 2(**V**)] to the initial form of the catalyst [cf. Scheme 2(**I**)] to start e new catalytic cycle for oxidation of benzyl alcohol with an aqueous H_2O_2.

The effect of solvent could be explained according to the proposed mechanistic aspects. The extraction of two water molecules in the steps (II) and (IV) in Scheme 2, might help to understand the nature of the catalytic behavior of the studied catalyst complexes. In the more polar solvent, e.g. acetonitrile, the catalytic process could be preceded homogenously due to the extracting of water molecules, whereas, in less polar solvent, the heterogeneous nature of the reaction media may reduce the catalytic chemoselectivity. The solubility of titled complex catalysts may also play an observable role in their catalytic potentials. They are sparingly soluble in dichloromethane and chloroform in which the catalytic ability of the current complex catalysts deactivated and exhibited very low yield of the oxidation process heterogeneously, especially with aqueous H_2O_2 [63].

The impact of the electronic and steric features of the Cunpap, Cubsisnph and Cunpisnph complexes on their stability and catalytic potential could be illustrated by the summarized catalytic results in Tables 3, 4 and 5 and Fig. 9a–c. Different structurally Cu^{2+} complexes were subjected to the oxidation of benzyl alcohol by an aqueous H_2O_2 have an observable impact by their steric effects [63]. This behavior has been widely reported and proved particularly by the electronic spectral scan of the oxidation processes [64. 65]. The order of catalytic activity was found to be Cubsisnph > Cupsisnph > Cunpap according to turnover frequency of the catalysts per various catalytic times (the optimized reaction time in Tables 3, 4, 5). As expected, a structural feature of complexes Cubsisnph and Cupsisnph complexes are less stable than Cunpap complex. Moreover, the *bis*-tridentate ligands in Cunpap form more close and stable catalyst complexes, which does not give any chance for the oxidant molecule or the substrate to approach to the central metal ion in step I of the suggested mechanism (Scheme 2). This feature of Cuapap complex decreases its catalytic potential of benzyl alcohol oxidation by an aqueous H_2O_2. This probably explains the low yield product of the chemoselective benzaldehyde catalyzed by Cunpap complex the oxidation of benzyl alcohol in in the optimized reaction conditions compared to that oxidation by Cubsisnph and Cupsisnph complexes in the optimized reaction conditions (Fig. 9a–c). In addition, the steric demands of the more reactive catalyst complexes Cubsisnph and Cupsisnph complexes which involve a more labile coordinated water molecule and a labile acetate ion in the coordination sphere. The water molecule or the acetate ion in Cubsisnph and Cupsisnph catalysts may allow more catalytic potential for the oxidation of benzyl alcohol and this also may explain the temperature needed oxidation processes for them. The more labile coordinated water molecule and acetate ion may facilitate the oxygen transfer from the oxidant, H_2O_2, to the catalyst complex, [Scheme 2 (**I**)], as observed previously [70]. The performing results for the activity and stability of these easily prepared current complexes during the oxidation reactions [cf. Scheme 2], leading to low/good conversion at reasonably low reaction

times with H_2O_2, along with good chemoselectivity conversion are strong advantages of the present Cu^{2+} complexes as oxidation catalysts [66].

6 Conclusion

The Schiff bases have been most widely utilized versatile ligands, in their neutral or deprotonated forms to form stable complexes with most of the transition metal ions especially with Cu(II) ion. The paper described the preparation and characterization of mononuclear Cu(II) Schiff base complexes. The structure of Schiff base ligands and their Cu(II) complexes has been comprehensively investigated. The newly synthesized Schiff base ligands act as tri and tetradentate ligands and coordinated to Cu(II) ion forming octahedral geometry. The catalytic abilities of these complexes were estimated using the environmentally friendly and clean oxidant H_2O_2 for the oxidation of benzyl alcohol. Cubsisnph shows excellent catalytic activity than Cunpisnph and Cunpap complexes. Furthermore, the effects of various parameters, including the molar ratio of catalyst to substrate, the temperature and the solvent, have been studied and optimized conditions were obtained. The best catalytic performance for the Cunpap, Cubsisnph and Cunpisnph complexes is observed in acetonitrile at 70 and 60 °C. The influence of molar ratio of catalyst to substrate deduced that by increasing the molar ratio of catalyst (0.02 to 1.00 mmol) increased their catalytic activity with decreasing their selectivity to carbonyl product (benzaldehyde). The effect of solvents could be given by the trend of catalytic and was ordered as acetonitrile > acetone > dichloromethane > chloroform > DMF.

References

1. Liu R, Liang X, Dong C, Hu X (2004) J Am Chem Soc 126:4112
2. Ferguson G, Ajjou AN (2003) Tetrahedron Lett 44:9139
3. Adam W, Gelalcha FG, Saha-Moller CR, Stegmann VR (2000) J Org Chem 65:1915
4. Menger FM, Lee C (1981) Tetrahedron Lett 22:1655
5. Rothenberg G, Feldberg L, Wiener H, Sasson Y (1998) J Chem Soc Perkin Trans 2:2429
6. Abu-Dief AM, Nassr LAE (2015) J Ira. Chem Soc 12:943–955
7. Corhnelissen JP, Van Diemen JH, Groeneveld LR, Hassnoot JG, Spek AL, Reedisk J (1992) Inorg Chem 31:198–202
8. Bianchini G, Crucianelli M, de Angelis F, Neri V, Saladino R (2005) Tetrahedron Lett 46:2427
9. Kumar A, Jain N, Chauhan SMS (2007) Synlett 41:411
10. Nan J, Arthur JR (2007) Tetrahedron Lett 48:273
11. Markó IE, Giles PR, Tsukazaki M, Chellé-Regnaut I, Gautier A, Brown SM, Urch CJ (1999) J Org Chem 64:2433
12. Ragagnin G, Betzemeier B, Quici S, Knochel P (2002) Tetrahedron 58:3985
13. Ansari IA, Gree R (2002) Org Lett 4:1507
14. Ramakrishna D, Bhat BR (2011) Inorg Chem Commun 14:690–693
15. Nan J, Arthur JR (2007) Tetrahedron Lett 48:411
16. Marko IE, Giles PR, Tsukazaki M, Chellę-Regnaut I, Gautier A, Brown SM, Urch CJ (1999) J Org Chem 64:2433
17. Abdel-Rahman LH, Abu-Dief AM, Ismael M, Mohamed MAA, Hashem NA (2016) J Mol Struct 1103:232–244
18. Abdel-Rahman LH, El-Khatib RM, Nassr LAE, Abu-Dief AM (2013) J Mole Struct. 1040:9–18
19. Abdel-Rahman LH, El-Khatib RM, Nassr LAE, Abu-Dief AM, Lashin FED (2013) J Spectrochim Acta A 111:266–276
20. Abdel-Rahman LH, Abu-Dief AM, Hamdan SK, Seleem AA (2015) Int J Nano Chem 1(2):65–77
21. Singh VP, Singh S, Singh DP (2012) J Enz Inh Med Chem 27 (3):319–329
22. Sheldrick, GM (1986). SHELXS86. Program for the solution of crystal structures. Univ. of Gottingen, Federal Republic of Germany
23. Abu-Dief AM, Díaz-Torres R, Sañudo EC, Abdel-Rahman LH, Alcalde NA (2013) Polyhedron 64:203–208
24. Abu-Dief AM, Abdelbaky MSM (2015) Garcia-Granda S Acta. Acta Cryst E 72:496–497
25. Betteridge PW, Carruthers JR, Cooper RI, Prout K, Watkin DJ (2003) J App Cryst 36:1487
26. Watkin DJ, Prout CK, Pearce LJ (1996) CAMERON. Chemical Crystallography Laboratory, Oxford
27. Abdel-Rahman LH, El-Khatib RM, Nassr LAE, Abu-Dief AM, Ismael M, Seleem AA (2014) J Spectrochim Acta A 117:366–378
28. Abd El-Lateef HM (2015) Abu-Dief AM, El-Gendy B E M. J Electroanal Chem 758:135–147
29. Mohamed GG, Zayed EM, Hindy AM (2015) Spectrochim Acta A 145:76–84
30. Frisch MJ, Trucks GW et al (2009) Gaussian 09, revision A. 02. Gaussian Inc, Wallingford
31. Becke AD (1993) J Chem Phys 98:5648
32. McGrath MP, Radom C (1991) J Chem Phys 94:511
33. Hay PJ, Wadt WR (1985) J Chem Phys 82:299
34. Ranganathan H, Ramaswamy D, Ramasami T, Santappa M (1979) Chem Lett 8:1201
35. Belal AAM, El-Deen IM, Farid NY, Zakaria R, Refat MS (2015) J Spectrochim Acta A 149:771–787
36. Gupta SK, Anjana C, Sen N, Butcher RJ, Jasinski JP, Golen JA (2015) Polyhedron 89:219–231
37. Lever ABP (1968) Inorganic electronic spectroscopy, 2nd edn. Elsevier, New York
38. Salavati-Niasari M, Salimi Z, Bazarganipour M, Davar F (2009) Inorg Chim Acta 362:3715
39. Tyagi M, Chandra S, Akhtar J, Chand D (2014) J Spectrochim Acta A 118:1056–1061
40. Abd El-Wahab ZH, Mashaly MM, Salman AA, El-Shetary BA, Faheim AA (2004) Spectrochim Acta A 60:2861
41. Nakamoto K (1970) Infrared spectra of Inorganic and Coordination Compounds. Willey, New York
42. Kovacic JE (1967) J Spectrochim Acta Part A 23:183–187
43. Pattanayak P, LalPratihar J, Patra D, Brandao P, Mal D, Felix V (2013) Polyhedron 59:23–28
44. Raman N, Sobha S (2012) Spectrochim Acta A 85:223–234
45. Thankamony M, Kumari BS, Rijulal G, Mohanan K (2009) J Therm Anal Cal 95:259–266
46. Neena S, Sunita H, Jyoti S, Vanita P, Agarwala BV (1992) Synth React Inorg Met Org Chem 22: 1283. (b) Murukan B, Mohanan K (2006). Transition Met Chem 31:441–446

47. Vogel AI (1994) A text book of quantitative inorganic analysis. Longmans, London
48. Nakamoto K (1985) Infrared and Raman spectra of Inorganic and coordination chemistry, part B, 5th edn. Wiley, New York, pp 87–98
49. Lever ABP (1984) Inorganic electronic spectroscopy, 2nd edn. Elsevier, New York
50. Ray D, Bharadwaj PK (2008) Inorg Chem 47:2252–2254
51. Ali OAM (2014) Spectrochim Acta, Part A 132:52–60
52. Ali OAM, El-Medani SM (2015) Abu Serea MR, Sayed ASS. Spectrochim Acta A 136:651–660
53. Asadi M, Asadi Z, Savaripoor N, Dusek M, Eigner V, Shorkaei MR, Sedaghat M (2015) Spectrochim Acta A 136:625–634
54. Khalaji AD, Rad SM, Grivani G, Das D (2011) J Therm Anal Calorim 103:747–751
55. Liu H, Wang H, Gao F, Niu D, Lu Z (2007) J Coord Chem 60:2671–2678
56. Keypour H, Shooshtari A, Rezaeivala M, Ozturkkup F, Rudbari HA (2015) Polyhedron 100:180–191
57. El-Asmy AA, Al-Ansi TY, Amine RR, Mounir MM (1990) Polyhedron 9:2029
58. Taakeyama T, Fx Quinn (1994) Thermal analysis, fundamentals and applications to polymer science. Wiley, Chichester
59. Frost AA, Pearson RG (1961) Kinetics and Mechanisms. Wiley, New York
60. El-Remaily AMAA, Abu-Dief AM (2015) Tetrahedron 71:2579–2584
61. Abu-Dief AM, Abdelbakyb MSM, Martínez-Blanco D, Amghouz Z, García-Granda S (2016) Mater Chem Phys 174:164–171
62. Zumdahl SS (2000) Chemistry for chemical and biological Science. University Science Books, USA
63. Adam MSS (2015) Monatsh Chem 146:1823–1836
64. Hosseini-Monfared H, Bikas R, Mayer P (2010) Inorg Chim Acta 363:2574
65. Noshiranzadeh N, Bikas R, Slepokura K, Mayeli M, Lis T (2014) Inorg Chim Acta 421:176–182
66. Bagherzadeh M, Zare M, Amani V, Ellern A, Woo LK (2013) Polyhedron 53:223
67. Rezaeifard A, Sheikhshoaie I, Monadi N, Alipour M (2010) Polyhedron 29:2703
68. Zueva E, Walton P, McGrady JE (2006) Dalton Trans 1:159–167
69. Kumar KN, Ramesh R (2005) Polyhedron 24:1885–1892
70. Banu KS, Chattopadhyay T, Banerjee A, Bhattacharya S, Zangrando E (2009) J Mol Catal. A 310:34–41
71. Ma L, Zhang Q, Cheng L, Wu Z, Yang J (2014) RSC Adv 4:30558–30565